**Electronic Supplementary Information**

# Benzylene-Linked [PNP] Scaffolds and Their Cyclometalated Zirconium and Hafnium Complexes

Malte Sietzen,‡ Sonja Batke,‡ Patrick W. Antoni, Hubert Wadepohl and Joachim Ballmann*

*Anorganisch-Chemisches Institut, Universität Heidelberg,*
*Im Neuenheimer Feld 276, 69120 Heidelberg, Germany.*

‡ These authors contributed equally to this work.

## Table of Contents

# 1) Additional Experimental Details

***Alternative Synthetic Procedure for the Preparation of $^{[B]}$2-Zr***

For the synthesis of $^{[B]}$**2-Zr**, an alternative synthetic pathway via the corresponding trichloride was developed. Upon reaction of [**B**]H with $ZrCl_4$ in the presence of $LiN(SiMe_3)_2$, [**B**]$ZrCl_3$ was generated and isolated in an analytically pure form. The latter trichloride was then reacted with $Me_3SiI$ to afford the desired triiodide $^{[B]}$**2-Zr** (see Scheme S1). Experimental procedures, complete characterization data and an ORTEP diagram of [**B**]$ZrCl_3$ (see Fig. S1) are provided below.

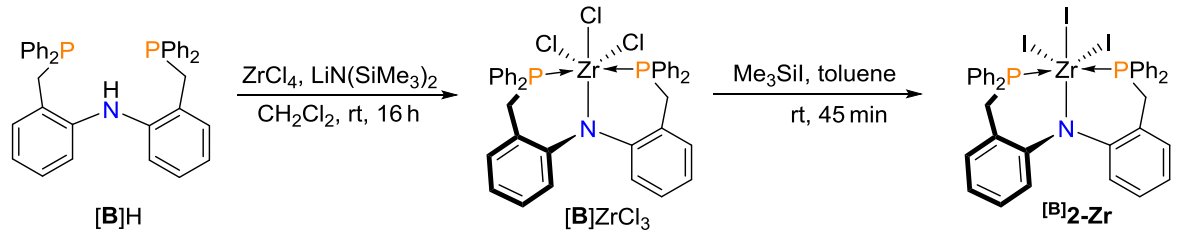


Scheme S1: Synthesis of $^{[B]}$**2-Zr** via the corresponding trichloride [**B**]$ZrCl_3$.

**[B]$ZrCl_3$**. Solid $ZrCl_4$ (0.22 g, 0.93 µmol, 1.10 eq.) was added to a solution of [**B**]H (0.50 g, 0.88 mmol, 1.00 eq.) in $CH_2Cl_2$ (30 mL) and the resulting suspension was stirred for 3 h at room temperature. Solid $LiN(SiMe_3)_2$ (148 mg, 0.884 mmol, 1.00 eq.) was added in one portion and stirring was continued for 16 h. The suspension was filtered through Celite and the Celite pad was washed with $CH_2Cl_2$ (10 mL). The filtrate was evaporated under reduced pressure, the residue was washed with cold toluene (10 mL, precooled to −40°C) and dried in vacuum to afford the product as a yellow powder (0.41 g, 0.54 mmol, 61 %). $^1$H NMR (600 MHz, $CD_2Cl_2$): $\delta$[ppm] = 7.51 (t, $^3J_{H,H}$ = 8.4 Hz, 8 H, *o*-PPh), 7.37 (t, $^3J_{H,H}$ = 7.4 Hz, 4 H, *p*-PPh), 7.31 (d, $^3J_{H,H}$ = 7.5 Hz, 2 H, H-5), 7.28 (dd, $^3J_{H,H}$ = 7.4 Hz, $^3J_{H,H}$ = 6.4 Hz, 8 H, *m*-PPh), 7.15 (m, 4 H, H-3 and H-4), 7.01 (d, $^3J_{H,H}$ = 7.3 Hz, 2 H, H-6), 3.44 (d, $^3J_{H,H}$ = 7.8 Hz, 4 H, $PCH_2$); $^{13}C\{^1H\}$ NMR (151 MHz, $CD_2Cl_2$): $\delta$ [ppm] = 139.2 ($s_{br}$, C-1), 133.1 ($s_{br}$, *ipso*-PPh), 131.5 (d, $^2J_{C,P}$ = 10.3 Hz, *o*-PPh), 131.4 (d, $^3J_{C,P}$ = 6.3 Hz, C-3), 130.4 (s, C-2), 130.2 (s, C-6), 129.0 (d, $^4J_{C,P}$ = 1.6 Hz, *p*-PPh), 128.5 (s, C-5), 127.3 (d, $^3J_{C,P}$ = 8.7 Hz, *m*-PPh), 126.2 (s, C-4), 27.1 (d, $^1J_{C,P}$ = 12.0 Hz, $PCH_2$); $^{31}P\{^1H\}$NMR (243 MHz, $CD_2Cl_2$): $\delta$[ppm] = −11.6 (s). Elemental analysis calcd. for $C_{38}H_{32}Cl_3NP_2Zr$: C 59.88, H 4.23, N 1.84; found: C 59.44, H 4.41, N 1.77.

**Synthesis of [B]$ZrI_3$ ($^{[B]}$2-Zr) starting from [B]$ZrCl_3$.** A stirred solution of **[B]$ZrCl_3$** (0.38 g, 0.50 mmol, 1.00 eq.) in $CH_2Cl_2$ (20 mL) was treated with iodotrimethylsilane (0.34 mg, 1.70 mmol, 3.40 eq.) and the resulting reaction mixture was stirred for 45 minutes at room temperature. The volume of the solvent was reduced to approximately 5 mL and the suspension was filtered over a sinter glass frit. The crude product was washed with cold $CH_2Cl_2$ (5 mL, precooled to −40 °C) and dried in vacuum to afford the title compound as an orange powder (0.28 mg, 0.27 mmol, 54 %). Analytical data are provided in the experimental section of the article.

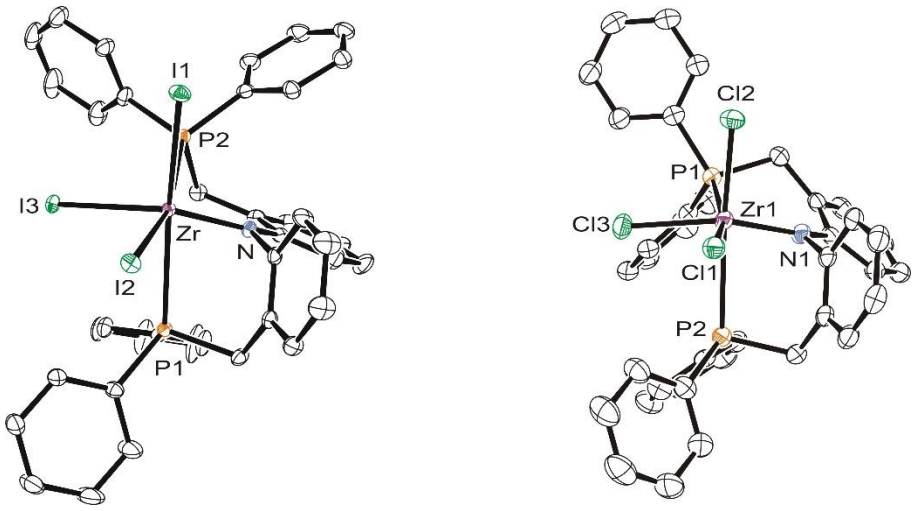


Fig. S1: ORTEP plot of the molecular structure of [**B**]ZrI$_3$ ([B]**2-Zr**) and [**B**]ZrCl$_3$ and (hydrogen atoms omitted for clarity, thermal ellipsoids set at 50 % probability). Selected bond lengths (Å) and angles (°) for [**B**]ZrI$_3$ ([B]**2-Zr**): I1–Zr 2.8727(8), I2–Zr 2.8265(11), I3–Zr 2.7959(9), Zr–P1 2.8357(8), Zr–P2 2.7661(12), Zr–N 2.0555(16), I2–Zr–I1 86.893(18), I3–Zr–I1 101.91(3), I3–Zr–I2 92.892(14), P2–Zr–P1 111.05(2), N–Zr–I1 108.19(5), N–Zr–I2 121.04(4), N–Zr–I3 134.91(4); selected bond lengths (Å) and angles (°) for [**B**]ZrCl$_3$: Zr1–Cl1 2.4490(5), Zr1–Cl2 2.4302(5), Zr1–Cl3 2.4630(5), Zr1–P1 2.8245(5), Zr1–P2 2.8417(5), Zr1–N1 2.0930(15), Cl1–Zr1–Cl3 90.696(16), Cl2–Zr1–Cl1 92.650(16), Cl2–Zr1–Cl3 99.654(17), P1–Zr1–P2 102.595(14), N1–Zr1–Cl1 116.62(4), N1–Zr1–Cl2 99.87(4), N1–Zr1–Cl3 145.36(4).

***Details on the Deuterium Labeling Experiments***

Starting from [**B**]ZrCl$_3$ and Bn$_2$Mg(OEt$_2$)$_2$, [B]**5-Zr** could be prepared readily, which was exploited for the synthesis of the deuterated derivatives [$^{PCNP}$**B**]ZrCl(CD$_2$Ph), [**B**]ZrCl($\eta^6$-C$_6$H$_5$-CHD$_2$) and [**B**-$d_1$]ZrCl($\eta^6$-C$_6$H$_5$-CD$_3$) (see Scheme S2). Due to their lower solubilities (see article text), this route failed when the corresponding triiodides [B]**2-M** (M = Zr, Hf) were employed as starting materials.

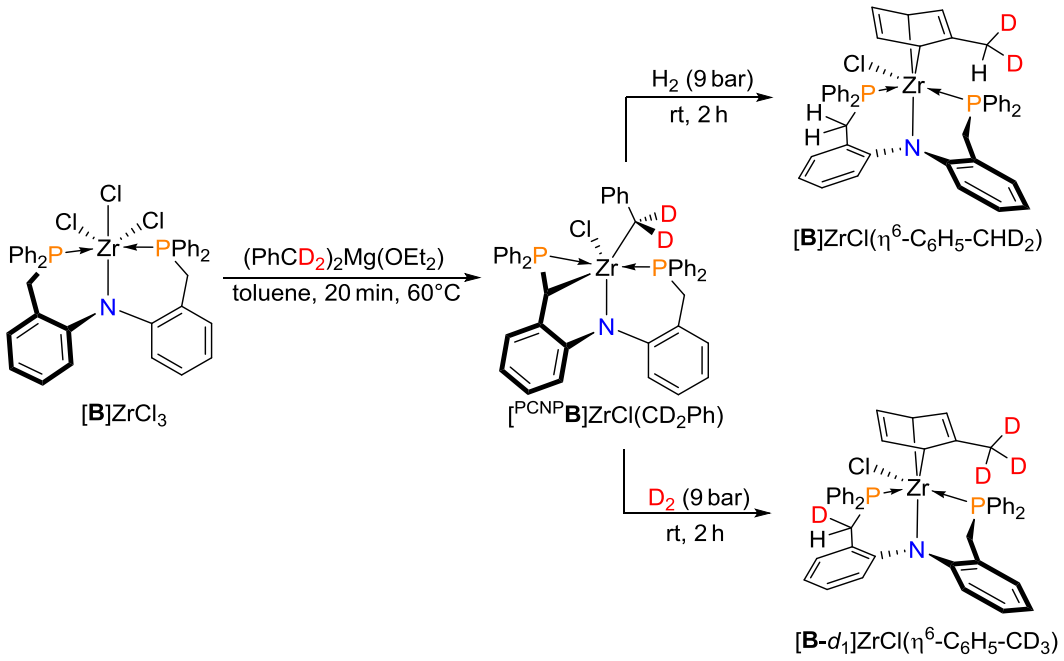


Scheme S2: Synthesis of [$^{PCNP}$**B**]ZrCl(CD$_2$Ph), [**B**]ZrCl($\eta^6$-C$_6$H$_5$-CHD$_2$) and [**B**-$d_1$]ZrCl($\eta^6$-C$_6$H$_5$-CD$_3$).

**[$^{PCNP}$B]ZrCl($CD_2Ph$).** To a suspension [**B**]$ZrCl_3$ (60 mg, 79 µmol, 1.00 eq.) in toluene (15 mL) was added a solution of $(PhCD_2)_2Mg(OEt_2)_2$ (30 mg, 84 µmol, 1.06 eq.) in toluene (3 mL) at room temperature. The reaction mixture was stirred for 20 minutes at 60 °C before removal of the solvent under reduced pressure. Toluene (5 mL) and 4 drops of dioxane were added to the residue and the resulting suspension was filtered through Celite. The filtrate was evaporated under reduced pressure and the residue was washed with pentane and dried in vacuum to afford the product as a yellow powder (44 mg, 57 µmol, 72 %). $^1$H NMR (400 MHz, tol-$d_8$): $\delta$ [ppm] = 8.36 - 8.19 (m, 2 H, Ar-H), 8.13 (t, *J* = 8.0 Hz, 2 H, Ar-H), 7.82 - 7.69 (m, 2 H, Ar-H), 7.23 (d, *J* = 8.2 Hz, 1 H, Ar-H), 7.20 - 7.10 (m, 4 H, Ar-H), 7.10 - 7.03 (m, 2 H, Ar-H), 7.00 (d, *J* = 0.9 Hz, 1 H, Ar-H), 6.96 - 6.88 (m, 3 H, Ar-H), 6.86 - 6.76 (m, 2 H, Ar-H), 6.72 (td, *J* = 1.3 Hz, *J* = 7.4 Hz, 1 H, Ar-H), 6.70 - 6.62 (m, 3 H, Ar-H), 6.57 (t, *J* = 7.3 Hz, 1 H, Ar-H), 6.46 (dt, *J* = 4.1 Hz, *J* = 7.9 Hz, 2 H, Ar-H), 6.43 - 6.31 (m, 3 H, Ar-H), 6.24 (d, *J* = 7.3 Hz, 2 H, Ar-H), 6.14 (t, *J* = 7.7 Hz, 1 H, Ar-H), 4.98 (d, *J* = 8.1 Hz, 1 H, Ar-H), 4.21 (s, *J* = 9.6 Hz, 1 H, PCH), 3.49 (dd, *J* = 11.7 Hz, *J* = 13.5 Hz, 1 H, $PCH_2$), 3.18 (d, *J* = 13.6 Hz, 1 H, $PCH_2$).

**[B]ZrCl($\eta^6$-$C_6H_5$-$CHD_2$).** A solution of [$^{PNCP}$**B**]ZrCl($CD_2Ph$) (44 mg, 57 µmol) in a mixture of toluene (0.4 mL) and $Et_2O$ (0.2 mL) was transferred to a thick-wall high-pressure NMR tube and pressurised with $H_2$ (9 bar). After keeping the sealed tube at room temperature for 2 h, the pressure was released and the solvent evaporated in vacuum. The residue was washed with pentane and dried in vacuum to afford the product as a dark green powder (31 mg, 39 µmol, 69 %). $^1$H NMR (400 MHz, tol-$d_8$, 233 K): $\delta$ [ppm] = 7.94 (t, *J* = 8.0 Hz, 2 H, Ar-H), 7.83 - 7.74 (m, 2 H, Ar-H), 7.20 (dd, *J* = 7.4 Hz, *J* = 13.5 Hz, 5 H, Ar-H), 7.13 - 7.08 (m, 3 H, Ar-H), 7.02 -7.00 (m, 1 H, Ar-H), 6.95 - 6.83 (m, 8 H, Ar-H), 6.78 (t, *J* = 7.2 Hz, 1 H, Ar-H), 6.75 - 6.67 (m, 2 H, Ar-H), 6.53 - 6.46 (m, 1 H, Ar-H), 6.18 (d, *J* = 8.0 Hz, 1 H, Ar-H), 5.95 (d, *J* = 17.5 Hz, 1 H, CH-Tol), 5.71 (d, *J* = 7.7 Hz, 1 H, Ar-H), 4.04 (dd, *J* = 5.7 Hz, *J* = 11.9 Hz, 1 H, CH-Tol), 3.78 - 3.58 (m, 3 H, $PCH_2$ and CH-Tol), 3.42 (dd, *J* = 7.7 Hz, *J* = 13.3 Hz, 1 H, $PCH_2$), 3.26 - 3.14 (m, 1 H, $PCH_2$), 3.13 - 3.03 (m, 2 H, $PCH_2$ and CH-Tol), 1.36 (s, 1 H, $CHD_2$).

**[B-$d_1$]ZrCl($\eta^6$-$C_6H_5$-$CD_3$).** A solution of [$^{PNCP}$**B**]ZrCl($CD_2Ph$) (44 mg, 57 µmol) in toluene (0.5 mL) was transferred to a thick-wall high-pressure NMR tube and pressurised with $D_2$ (9 bar). After keeping the sealed tube at room temperature for 2 h, the pressure was released and the solvent evaporated in vacuum. The residue was washed with pentane and dried in vacuum to afford the product as a dark green powder (32 mg, 41 µmol, 72 %). $^1$H NMR (400 MHz, tol-$d_8$, 233 K): $\delta$ [ppm] = 7.92 (t, *J* = 7.9 Hz, 2 H, Ar-H), 7.82 - 7.75 (m, 2 H, Ar-H), 7.23 - 7.16 (m, 5 H, Ar-H), 7.10 - 6.96 (m, 7 H, Ar-H), 6.93 - 6.83 (m, 5 H, Ar-H), 6.80 - 6.67 (m, 3 H, Ar-H), 6.53 - 6.46 (m, 1 H, Ar-H), 6.16 (d, *J* = 8.1 Hz, 1 H, Ar-H), 5.93 (d, *J* = 13.7 Hz, 1 H, CH-Tol), 5.70 (d, *J* = 7.4 Hz, 1 H, Ar-H), 4.07 - 3.99 (m, 1 H, CH-Tol), 3.73 - 3.59 (m, 2 H, CH-Tol), 3.47 - 3.35 (m, 1 H, $PCH_2$), 3.25 - 3.14 (m, 1 H, $PCH_2$), 3.13 - 3.03 (m, 2 H, $PCH_2$ and CH-Tol).

***Details on the Synthesis of [A]5-Zr and its Hydrogenation Chemistry***

In the article, it is mentioned that partial alkylation of [**A**]$ZrI_3$ ([A]**2-Zr**) with $Bn_2Mg(OEt_2)_2$ (1 eq.) led to the formation of $\kappa^4$-[PCNP]ZrBnI ([A]**5-Zr**, see Scheme S3) along with an unidentified bi-product. Heating the former reaction mixture only very briefly (5 min, 70 °C, pre-heated oil-bath) gave the best results with only 10 - 15 % of the bi-product being formed. Two mutually coupled $^{31}P\{^1H\}$ NMR doublets at 11.7 and 30.1 ppm were found for the latter bi-product (see Figure S2). On basis of $^{31}P\{^1H\}$ NMR spectroscopy, it can be excluded that this bi-product corresponds to $\kappa^4$-[PCNP]$ZrBn_2$ ([A]**4-Zr**), as two doublets at 20.2 and 1.0 ppm were detected for [A]**4-Zr** (see Figure S2). Thus, it seems likely that the bi-product corresponds to $\kappa^4$-[PCNP]$ZrI_2$. When the amount of $Bn_2Mg(OEt_2)_2$ was increased to 1.2 eq., [A]**4-Zr** was formed as an additional product. The main product, $\kappa^4$-[PCNP]ZrBnI ([A]**5-Zr**), however, was identified unambiguously. In the $^1H$ NMR spectrum, one benzylic proton of the ligand's backbone was found to be absent. By $^{13}C$ DEPT, $^{13}C,^1H$ HSQC and $^{13}C\{^1H\}$ NMR spectroscopy, the remaining three benzylic protons of the ligand were assigned to one CH and one $CH_2$ group. The $^1H$ NMR signals corresponding to the metal-bound $CH_2$ unit of the benzyl substituent were detected at 2.75 and 2.41 ppm with an integral of one proton each.

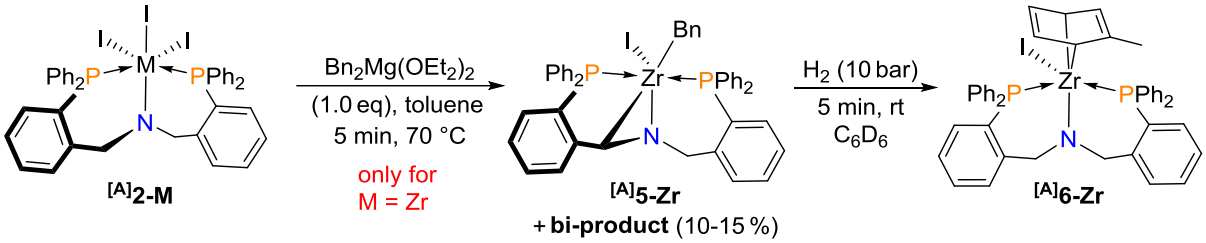


Scheme S3: Synthesis and hydrogenation of [A]**5-Zr**.

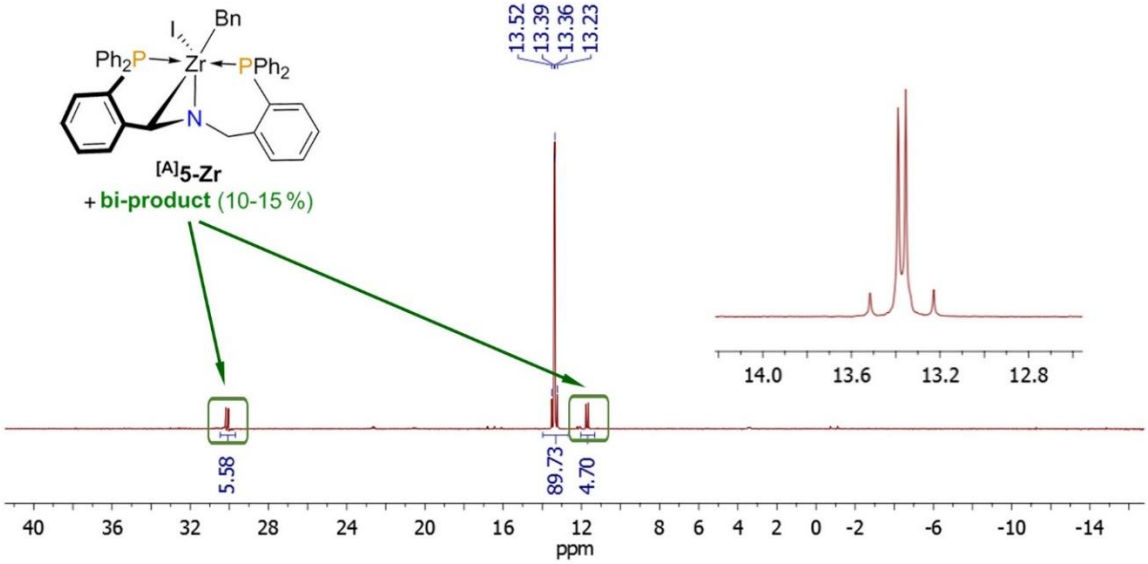


Fig. S2: $^{31}P\{^1H\}$ NMR (243 MHz, $C_6D_6$) of impure [A]**5-Zr**.

When a sample of [A]**5-Zr** (containing the above mentioned impurity) was subjected to dihydrogen (10 bar) at room temperature, an immediate colour change from yellow to brown-orange was observed. After work-up and re-crystallization, a product with only one $^{31}P\{^1H\}$ NMR resonance at 6.4 ppm was isolated. According to $^{31}P\{^1H\}$ NMR spectroscopy, no other phosphorus-containing species were present in the isolated sample, but the $^1H$ NMR spectrum revealed the presence of several minor unidentified impurities. Nevertheless, the resulting complex could be identified as [A]**6-Zr** (see Scheme

S3), although single crystals for X-ray diffraction were not obtained in numerous attempts. In the $^{1}$H NMR spectroscopy of $^{[A]}$**6-Zr**, two $CH_2$ groups were detected at and unambiguously assigned to the ligand's linkers by two-dimensional NMR techniques ($^{1}$H,$^{1}$H COSY, $^{13}$C,$^{1}$H HSCQ and $^{13}$C,$^{1}$H HMBC spectroscopy). The methyl group of the $\eta^6$-$C_7H_8$ moiety was detected in the $^{1}$H NMR spectrum as a singlet at 2.11 ppm. The $^{1}$H NMR resonances of the $\eta^6$-$C_7H_8$-ring protons were found at 4.48, 4.15 and 3.44 ppm in an approximate ratio of 1:2:2. A $^{1}$H NMR spectrum recorded *in situ* in shown in Figure S3. Experimental details are provided below.

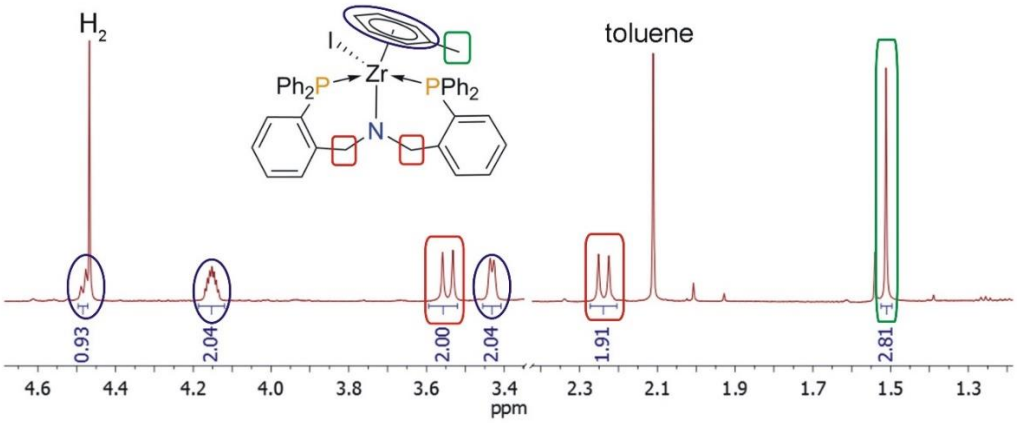


Fig. S3: *In situ* $^{1}$H NMR (243 MHz, $C_6D_6$) spectrum of $^{[B]}$**6-Zr**.

$^{[A]}$**5-Zr.** To a solution of the $^{[A]}$**2-Zr** (0.10 g, 0.10 mmol, 1.00 eq.) in toluene (10 mL) was added $Bn_2Mg(OEt_2)_2$ (34 mg, 0.10 mmol, 1.00 eq.) and the resulting reaction mixture was heated to 70 °C for 5 minutes in a pre-heated oilbath. The solvent was removed under reduced pressure and diethylether (3 mL) was added to solid residue. The mixture was filtered through a syringe filter and the filtrate evaporated to dryness. The residue was washed with pentane (3 mL) and dried in vacuum to afford the title compound as a dark orange powder (approximately 55 mg). As mentioned in the text, the material contained 10 - 15 % of a bi-product (presumably $\kappa^4$-[PCNP]$ZrI_2$), which could not be separated. Significantly higher percentages of this bi-product were observed upon scale-up. $^{1}$H NMR (600 MHz, $C_6D_6$): $\delta$ [ppm] = 8.20 (t, *J* = 7.9 Hz, 2 H, Ar-H), 7.67 (t, *J* = 7.7 Hz, 2 H, Ar-H), 7.47 - 7.52 (m, 2 H, Ar-H), 7.40 (t, *J* = 7.6 Hz, 2 H, Ar-H), 7.28 - 7.32 (m, 2 H, Ar-H), 7.24 (t, *J* = 8.3 Hz, 4 H, Ar-H), 7.20 (d, *J* = 7.4 Hz, 2 H, Ar-H), 7.11 - 6.93 (m, 8 H, Ar-H), 6.88 (t, *J* = 7.7 Hz, 2 H, Ar-H), 6.79 (t, *J* = 7.6 Hz, 2 H, Ar-H), 6.76 (d, *J* = 7.3 Hz, 1 H, Ar-H), 6.70 (t, *J* = 7.5 Hz, 2 H, Ar-H), 6.31 (dd, *J* = 7.7 Hz, *J* = 5.5 Hz, 1 H, Ar-H), 6.30 (d, *J* = 7.4 Hz, 1 H, Ar-H), 4.30 - 4.38 (m, 2 H, $NCH_2$), 3.27 (s, 1 H, NCH), 2.75 (dd, *J* = 9.8 Hz, *J* = 2.1 Hz, 1 H, Zr-$CH_2$), 2.41 (d, *J* = 7.2 Hz, 1 H, Zr-$CH_2$); $^{13}$C{$^{1}$H} NMR (151 MHz, $C_6D_6$): $\delta$ [ppm] = 159.2 (d, *J* = 27.2 Hz, Ar-C), 144.4 (d, *J* = 18.2 Hz, Ar-C) 135.9 (dd, *J* = 13.2 Hz, *J* = 3.1 Hz, Ar-C), 134.6 (d, *J* = 3.2 Hz, Ar-C), 134.5 (d, *J* = 2.6 Hz, Ar-C), 134.1 (d, *J* = 2.3 Hz, Ar-C), 134.0 (d, *J* = 2.4 Hz, Ar-C), 133.7 (d, *J* = 2.8 Hz, Ar-C), 133.6 (d, *J* = 2.9 Hz, Ar-C), 132.7 (t, *J* = 3.0 Hz, Ar-C), 130.8 (s, Ar-C), 130.6 (s, Ar-C), 130.2 (s, Ar-C), 130.0 (s, Ar-C), 129.8 (s, Ar-C), 129.3 (s, Ar-C), 129.1 (s, Ar-C), 129.0 (s, Ar-C), 128.6 (dd, *J* = 3.5 Hz, *J* = 1.5 Hz, Ar-C), 128.6 (d, *J* = 1.8 Hz, Ar-C), 128.4 (s, Ar-C), 128.2 (s, Ar-C), 125.6 (s, Ar-C), 125.3 (s, Ar-C), 128.4 (s, Ar-C), 124.3 (s, Ar-C), 124.2 (s Ar-C), 76.2 ($s_{br}$, NCH), 61.9 (d, *J* = 6.5 Hz, $CH_2$), 72.3 ($s_{br}$, Zr-$CH_2$); $^{31}$P{$^{1}$H} NMR (243 MHz, $C_6D_6$): δ [ppm] = 13.2 - 13.5 (two overlapping doublets); Elemental analysis was not attempted due to the presence of the bi-product (*vide supra*).

**[A]6-Zr.** A thick-wall NMR tube was charged with a solution of **[A]5-Zr** (40 mg) in $C_6D_6$ (0.5 mL) and pressurised with $H_2$ (10 bar). After one minute, the solvent was removed in vacuum and the residue recrystallised from $Et_2O$ (1 mL) to afford the product as a dark orange powder (15 mg). As stated in the text, **[A]5-Zr** contained an impurity, which disallows for the determination of a yield. $^1$H NMR (600 MHz, $C_6D_6$): $\delta$ [ppm] = 8.05 - 8.10 (m, 4 H, Ph-H), 7.47 - 7.51 (m, 3 H, H-3, Ph-H), 7.28 ($s_{br}$, 2 H, Ph-H), 7.17 - 7.22 (m, 6 H, H-4 and Ph-H), 6.91 - 7.09 (m, 13 H, H-5 and H-6 and Ph-H), 4.48 (t, $J$ = 7.5 Hz, 1 H, $\eta^6$-$C_7H_8$), 4.15 (sept, $J$ = 3.5 Hz, 2 H, $\eta^6$-$C_7H_8$), 3.54 (d, $J$ = 15.9 Hz, 2 H, $NCH_2$), 3.44 (d, $J$ = 5.6 Hz, 2 H, $\eta^6$-$C_7H_8$), 2.23 (d, $J$ = 15.9 Hz, 2 H, $NCH_2$), 2.11 (s, 3 H, $\eta^6$-$C_7H_8$-$CH_3$); $^{13}$C{$^1$H} NMR (151 MHz, $C_6D_6$): $\delta$ [ppm] = 153.2 (d, $J$ = 20.2 Hz, C-2), 148.1 (d, $J$ = 16.4 Hz, Ph-C), 135.0 (t, $J$ = 6.0 Hz, C-3), 134.1 (s, C-4), 133.5 (t, $J$ = 6.2 Hz, Ph-C), 129.1 (d, $J$ = 16.7 Hz, C-1), 129.0 (s, Ph-C), 128.9 (s, C-6), 128.1 (s, Ph-C), 127.3 (t, $J$ = 2.2 Hz, C-5), 106.5 (d, $J$ = 2.5 Hz, C-10), 99.0 (s, C-9), 98.9 (s, C-8), 91.1 (s, C-7), 53.9 (t, $J$ = 3.0 Hz, $CH_2$), 21.1 (s, Tol-$CH_3$); $^{31}$P{$^1$H} NMR (243 MHz, $C_6D_6$): $\delta$ [ppm] = 6.4 (s); Elemental analysis was not attempted due to the presence of impurities in the aromatic region of the $^1$H NMR spectrum (*vide supra*).

## ***The $^i$Pr- and $^t$Bu-Derivatives of [B]H: Synthesis and Preliminary Complexation Experiments***

It is mentioned in the article that the $^i$Pr$_2$P- and $^t$Bu$_2$P-derivatives of [**B**]H have been prepared as well. In both cases, the borane-protected phosphines $R_2PH(BH_3)$ (R = $^i$Pr, $^t$Bu) were reacted with **5** (see Scheme S4) as the parent secondary phosphines $R_2PH$ failed to react cleanly. After deprotection, the target molecules were obtained as a colourless oil (R = $^i$Pr) and an off-white solid (R = $^t$Bu), respectively. Experimental details are provided below.

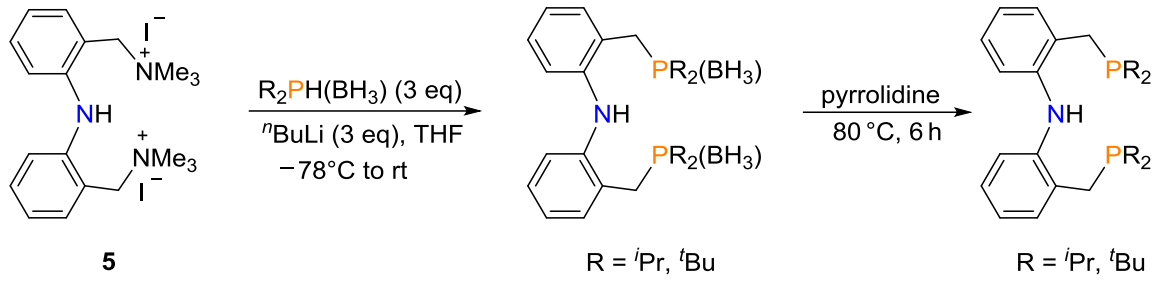


**5** R = $^i$Pr, $^t$Bu R = $^i$Pr, $^t$Bu

Scheme S4: Synthesis of $^{iPr}$[**B**]H and $^{tBu}$[**B**]H

**$^{iPr}$[B]H**. A solution of $^n$BuLi (18.8 mL, 2.5 M in hexane, 47.0 mmol, 3.50 eq.) was added dropwise to a stirred solution of $^i$Pr$_2$PH(BH$_3$) (5.32 g, 40.3 mmol, 3.00 eq.) in THF (100 mL) at 0°C. The resulting pale yellow solution was allowed to warm to room temperature and stirred for 5 h. The solution was cooled to –78 °C and solid **5** (7.62 g, 13.4 mmol, 1.00 eq.) was added in small portions. Once the addition was completed, the resulting reaction mixture was stirred for 30 minutes at –78 °C. The cooling bath was removed and stirring was continued for 12 h at room temperature. The reaction was quenched by the addition of water (100 mL) and $CH_2Cl_2$ (200 mL). The organic layer was separated and the aqueous layer was extracted twice with $CH_2Cl_2$. The combined organic fractions were dried over $MgSO_4$ and evaporated under reduced pressure. The residue was taken up in $CH_2Cl_2$ and filtered through silica. Crystallization from pentane at –25 °C afforded the borane-protected ligand as an off-white solid

(4.52 g, 9.89 mmol, 74 %). $^{1}$H NMR (600 MHz, $CDCl_3$): $\delta$ [ppm] = 7.31 (d, $^{3}J_{H,H}$ = 7.6 Hz, 2 H, 6-ArH), 7.11 (t, $^{3}J_{H,H}$ = 7.6 Hz, 2 H, 4-ArH), 6.94 (t, $^{3}J_{H,H}$ = 7.5 Hz, 2 H, 5-ArH), 6.90 (d, $^{3}J_{H,H}$ = 8.0 Hz, 2 H, 3-ArH), 6.49 (s, 1 H, NH), 3.12 (d, $^{2}J_{H,P}$ = 11.8 Hz, 4 H, $PCH_2$), 2.12 - 2.03 (m, 4 H, $^{i}$PrCH), 1.20 - 1.13 (m, 24 H, $^{i}PrCH_3$), 0.2 - 0.8 (m, 6 H, $BH_3$); $^{13}C\{^{1}H\}$ NMR(151 MHz MHz, $CDCl_3$): $\delta$ [ppm] = 143.4 (d, $^{3}J_{C,P}$ = 3.9 Hz, C-1), 131.9 (d, $^{4}J_{C,P}$ = 3.6 Hz, 6-ArC), 128.1 (d, $^{4}J_{C,P}$ = 2.4 Hz, 4-ArC), 124.8 (d, $^{2}J_{C,P}$ = 4.8 Hz, 2-ArC), 122.0 (d, $^{5}J_{C,P}$ = 2.1 Hz, 5-ArC), 120.9 (d, $^{3}J_{C,P}$ = 1.9 Hz, 3-ArC), 23.8 (d, $^{1}J_{C,P}$ = 28.7 Hz, $PCH_2$), 22.2 (d, $^{1}J_{C,P}$ = 31.8 Hz, $^{i}$PrCH), 17.3 (d, $^{2}J_{C,P}$= 18.2 Hz, $^{i}PrCH_3$); $^{11}B\{^{1}H\}$ NMR (193 MHz, $CDCl_3$): $\delta$ [ppm] = −42.5 (d, $^{1}J_{H,P}$ = 44.5 Hz); $^{31}P\{^{1}H\}$ NMR (242.9 MHz, $CDCl_3$): $\delta$ [ppm] = 34.8 - 34.4 (m). The borane-protected ligand (1.00 g, 2.19 mmol) was dissolved in pyrrolidine (20 mL) and the resulting solution was heated to 80 °C for 6 h. The solvent was evaporated under reduced pressure and the residue was taken up in pentane. The resulting solution was washed twice with degassed water and dried over $Na_2SO_4$. After filtration and evaporation, the residue was carefully dried in vacuum to afford the title compound as a viscous liquid (0.71 g, 1.65 mmol, 75 %). $^{1}$H NMR (600MHz, $C_6D_6$): $\delta$ [ppm] = 7.33 (d, $^{3}J_{H,H}$ = 7.6 Hz, 2 H, 6-ArH), 7.26 (d, $^{3}J_{H,H}$ = 8.01, 2 H, 3-ArH), 7.04 - 7.00 (m, 3 H, NH and 4-ArH), 6.87 (t, $^{3}J_{H,H}$ = 7.4, 2 H, 5-ArH), 2.88 (s, 4 H, $PCH_2$), 1.63(d of sept, $^{3}J_{H,H}$= 2.23 Hz, $^{2}J_{H,P}$= 16.5 Hz, 4 H, $^{i}$PrCH), 1.04 - 0.99 (m, 24 H, $^{i}PrCH_3$); $^{13}C\{^{1}H\}$ NMR (151 MHz, $C_6D_6$): $\delta$ [ppm] = 142.5 (s, 1-ArC), 131.2 (m, 6-ArC), 128.9 (m, 2-ArC), 126.8 (s, 4-ArC), 121.0 (s, 5-ArC), 119.0 (s, 3-ArC), 26.6 - 26.8 (m, $PCH_2$), 23.5 - 23.3 (m, $^{i}$PrCH), 19.5 - 19.2 (m, $i$PrCH$_3$); $^{31}P\{^{1}H\}$ NMR (243 MHz, $C_6D_6$): $\delta$ [ppm] = −0.3 (s); Elemental analysis calcd. for $C_{26}H_{41}NP_2$: C 72.70, H 9.62, N 3.26, found: C 72.71, H 9.61, N 3.35.

**$^{tBu}$[B]H**. A solution of $^{n}$BuLi (5.50 mL, 2.5 hexane, 13.75 mmol, 3.30 eq.) was added dropwise to a stirred solution of $^{t}Bu_2PH(BH_3)$ (2.00 g, 12.5 mmol, 3.00eq.) in THF (100 mL) at 0 °C. The resulting solution was allowed to warm to room temperature and was stirred for 5 h. The solution was cooled to –78 °C and solid **5** (2.36 g, 4.17 mmol, 1.00 eq.) was added in small portions. After stirring for 30 minutes at –78 °C, the mixture was warmed to room temperature and stirring was continued for 12 h. Following the work-up procedure provided for the $^{i}Pr_2P$-derivative, afforded the borane-protected product as a white solid (1.83 g, 3.56 mmol 86 %). $^{1}$H NMR (600MHz, $CDCl_3$): δ [ppm] = 7.59 (d, $^{3}J_{H,H}$ = 7.74 Hz, 2 H, 6-ArH), 7.10 (t, $^{3}J_{H,H}$ = 7.65 Hz, 2 H, 4-ArH), 6.93 (t, $^{3}J_{H,H}$ =7.50 Hz, 2 H, 5-ArH), 6.85 (m, 3 H, 3-ArH and NH), 3.18 (d, $^{2}J_{P,H}$= 12.2 Hz, 4 H, $PCH_2$), 1.26 (d, $^{3}J_{P,H}$ = 12.4 Hz, 36 H, $^{t}$Bu), 1.00 - 0.30 (m, 6 H, $BH_3$); $^{13}C\{^{1}H\}$ NMR (151 MHz, $CDCl_3$): δ [ppm] = 143.7 (d, $^{3}J_{C,P}$ = 4.0 Hz, 1-ArC), 132.5 (d, $^{4}J_{C,P}$ =3.3 Hz, 6-ArC), 128.0 (d, $^{4}J_{C,P}$ = 2.1 Hz, 4-ArC), 126.1 (d, $^{2}J_{C,P}$ =3.8 Hz, 2-ArC), 121.8 (d, $^{5}J_{C,P}$ =1.7 Hz, 5-ArC), 121.1 (d, $^{3}J_{C,P}$ =1.6 Hz, 3-ArC), 33.2 (d, $^{1}J_{C,P}$ =25.3 Hz, $^{t}BuC^{quart}$), 28.0 (d, $^{2}J_{C,P}$=0.9 Hz, $^{t}BuCH_3$), 21.5 (d, $^{1}J_{C,P}$ =25.6 Hz, $PCH_2$); $^{11}B\{^{1}H\}$ NMR (193 MHz, $CDCl_3$): δ [ppm] = −41.1 (s); $^{31}P\{^{1}H\}$ NMR (243 MHz, $CDCl_3$): δ [ppm] = 48.0 - 46.0 (m). A solution of the borane-protected ligand (1.00 g 1.95 mmol) in pyrrolidine (20 mL) was heated to 80 °C for 6 h in a sealed ampule under an atmosphere of dry argon. The solvent was evaporated under reduced pressure and the residue was washed with degassed water (2 × 10 mL). After prolonged drying in vacuum, the product was obtained as a colourless powder (0.83 g, 1.72 mmol, 88 %). $^{1}$H NMR (600MHz, $C_6D_6$): δ [ppm] = 7.5 - 7.6 (m, 3 H, 6-ArH and NH), 7.29 (d, $^{3}J_{H,H}$ = 7.3 Hz, 2 H, 3-ArH), 7.01 (t, $^{3}J_{H,H}$ = 7.07 Hz, 2 H, 4-ArH), 6.89 (t, $^{3}J_{H,H}$ = 7.0 Hz, 2 H, 5-ArH), 2.98 (d, $^{2}J_{H,P}$ = 1.8 Hz, 4 H, $PCH_2$), 1.11 (d, $^{3}J_{H,P}$ = 10.8 Hz, 36 H, $^{t}BuCH_3$); $^{13}C\{^{1}H\}$ NMR (151 MHz, $C_6D_6$): δ [ppm] = 124.8 (s, 1-ArC), 132.1 (d, $^{4}J_{C,P}$ = 11.3 Hz, 6-ArC), 130.1 (d, $^{2}J_{C,P}$ = 8.6 Hz, 2-ArC), 126.8 (d, $^{4}J_{C,P}$ = 1.6 Hz, 4-ArC), 121.1 (s, 5-ArC), 118.7 (s, 3-ArC), 32.0 (d, $^{1}J_{C,P}$ = 22.5, $^{t}BuC^{quart}$), 29.9 (d, $^{2}J_{C,P}$ = 13.0 Hz, $^{t}BuCH_3$), 25.6 (d, $^{1}J_{C,P}$ = 24.1 Hz, $PCH_2$); $^{31}P\{^{1}H\}$ NMR (243 MHz, $C_6D_6$): δ [ppm] = 23.0 (s); Elemental analysis calcd. for $C_{30}H_{49}NP_2$: C 74.19, H 10.17, N 2.88, found: C 74.21, H 10.02, N 2.98.

Preliminary experiments indicated that $^{iPr}$[**B**]H and $^{tBu}$[**B**]H are both well-suited for the preparation of zirconium complexes. Although an in-depth study is still pending, significantly different complex geometries and reactivities have been observed already: The trichloride $^{iPr}$[**B**]$ZrCl_3$, for example, was found to attain an octahedral structure (see Scheme S5 and Fig. S4), which is not the case for [**B**]$ZrCl_3$ (see Fig. S1). In $^{tBu}$[**B**]$ZrCl(Bn)_2$, only one sidearm of the ligand was found to coordinate to the metal in solution and in the solid state. So far, cyclometalation has not been observed for complexes bearing the sterically demanding $^{t}Bu_2P$-subsituted ligand. Clearly, further studies are required to elucidate these preliminary findings.

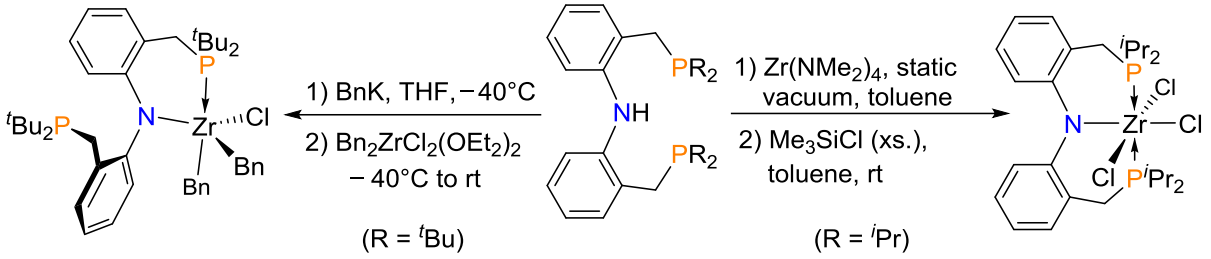


Scheme S5: Preliminary complexation studies with $^{iPr}$[**B**]H and $^{tBu}$[**B**]H.

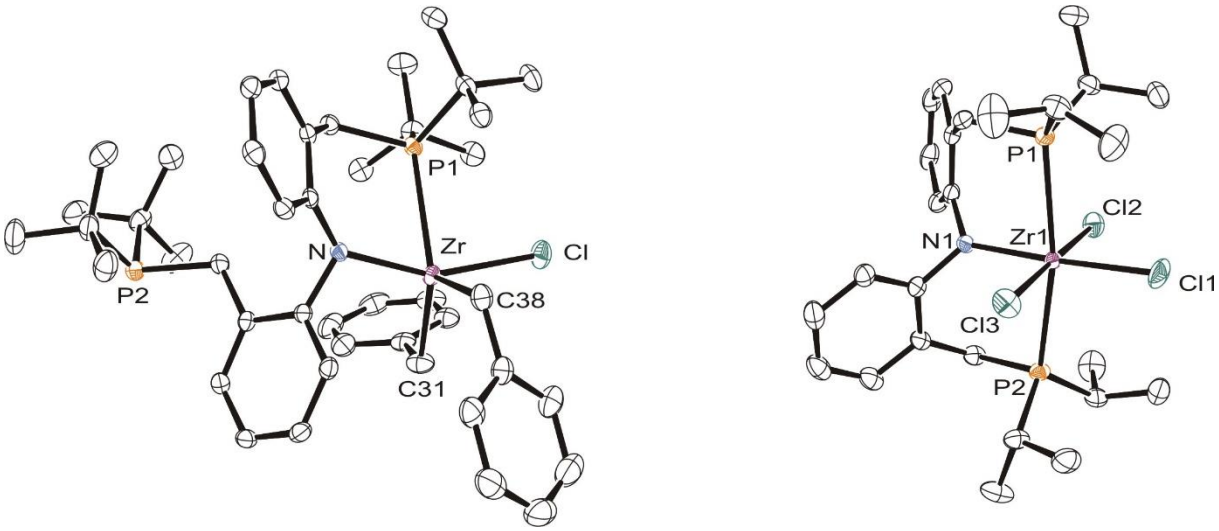


Fig. S4: ORTEP plots of the molecular structures of $^{tBu}$[**B**]$ZrCl(Bn)_2$ and $^{iPr}$[**B**]$ZrCl_3$ (hydrogen atoms omitted for clarity, thermal ellipsoids set at 50 % probability). Full details will be reported in due course.

## 3) Selected NMR Spectra

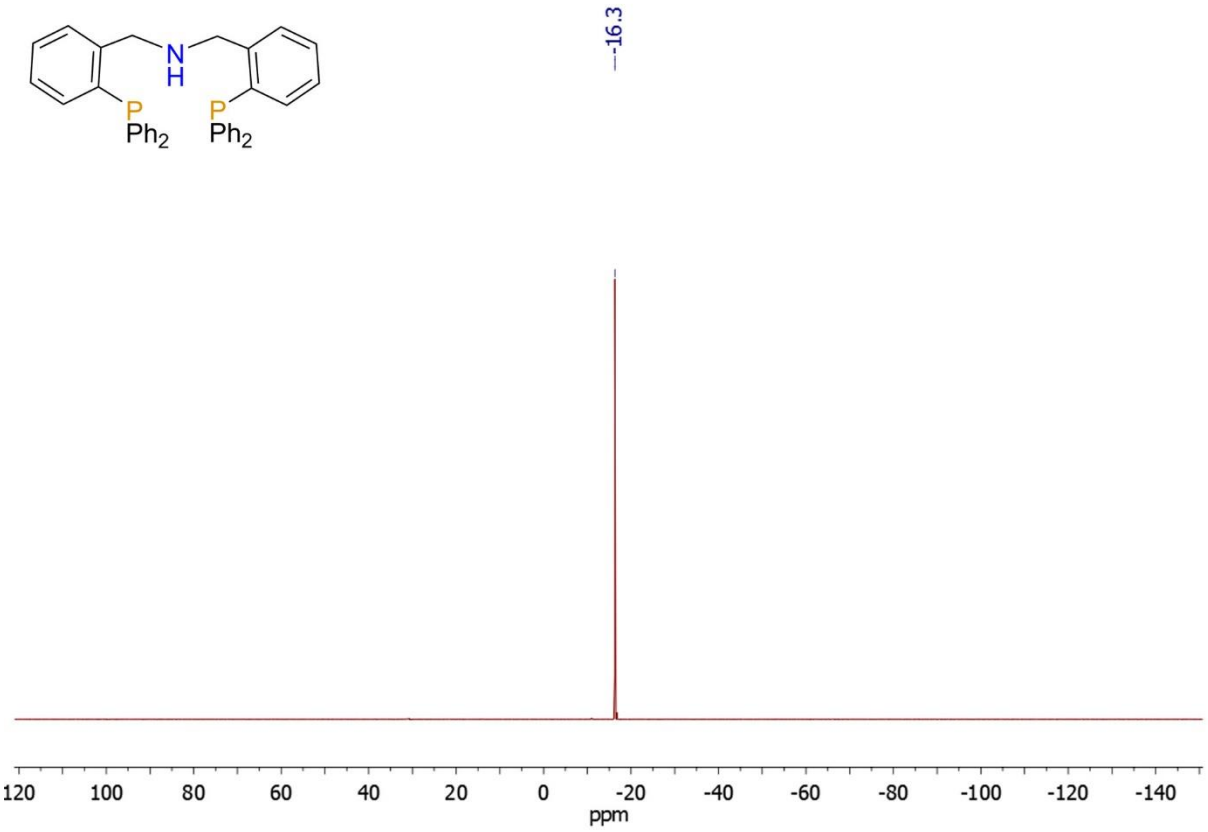


Fig. S5: $^{31}P\{^{1}H\}$ NMR (243 MHz, $CD_2Cl_2$) of [**A**]H.

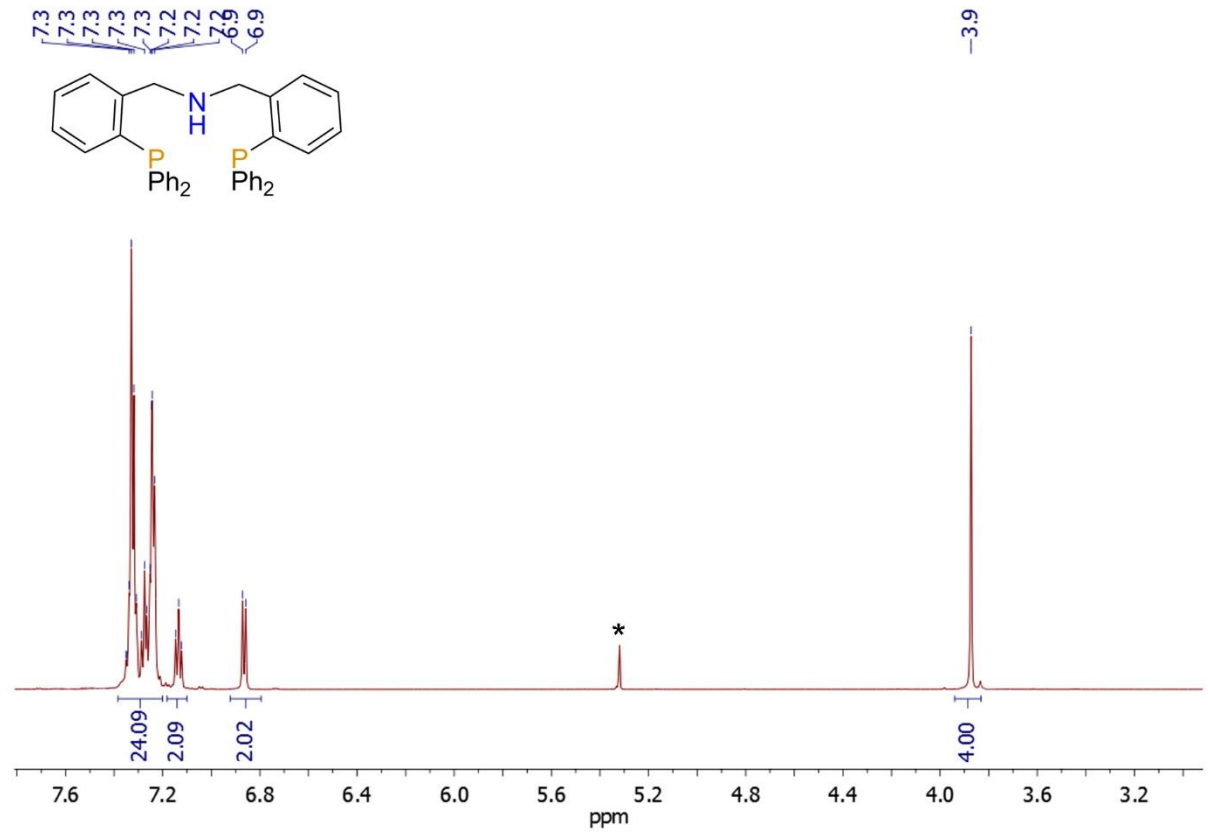


Fig. S6: $^{1}H$ NMR (600 MHz, $CD_2Cl_2$) of [**A**]H (residual proton signal of $CD_2Cl_2$ are labeled with ∗).

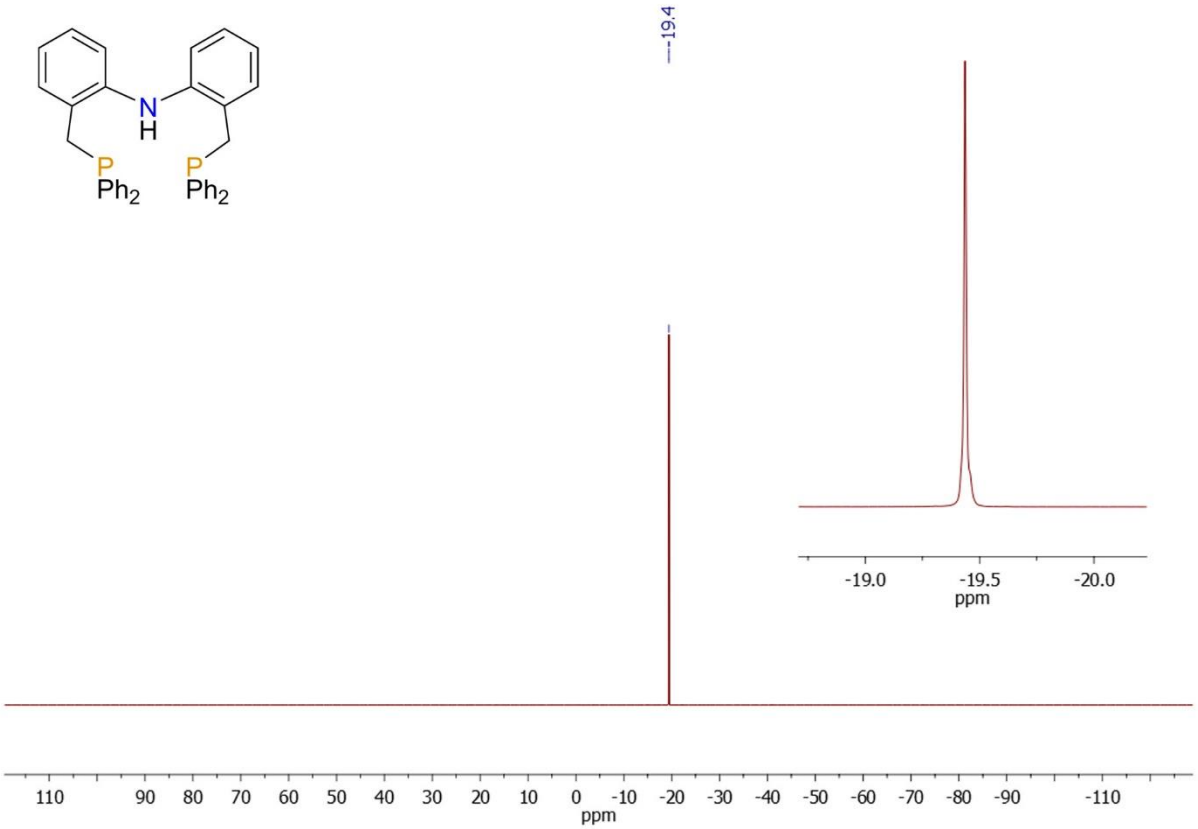


Fig. S7: $^{31}P\{^{1}H\}$ NMR (243 MHz, $C_6D_6$) of [**B**]H.

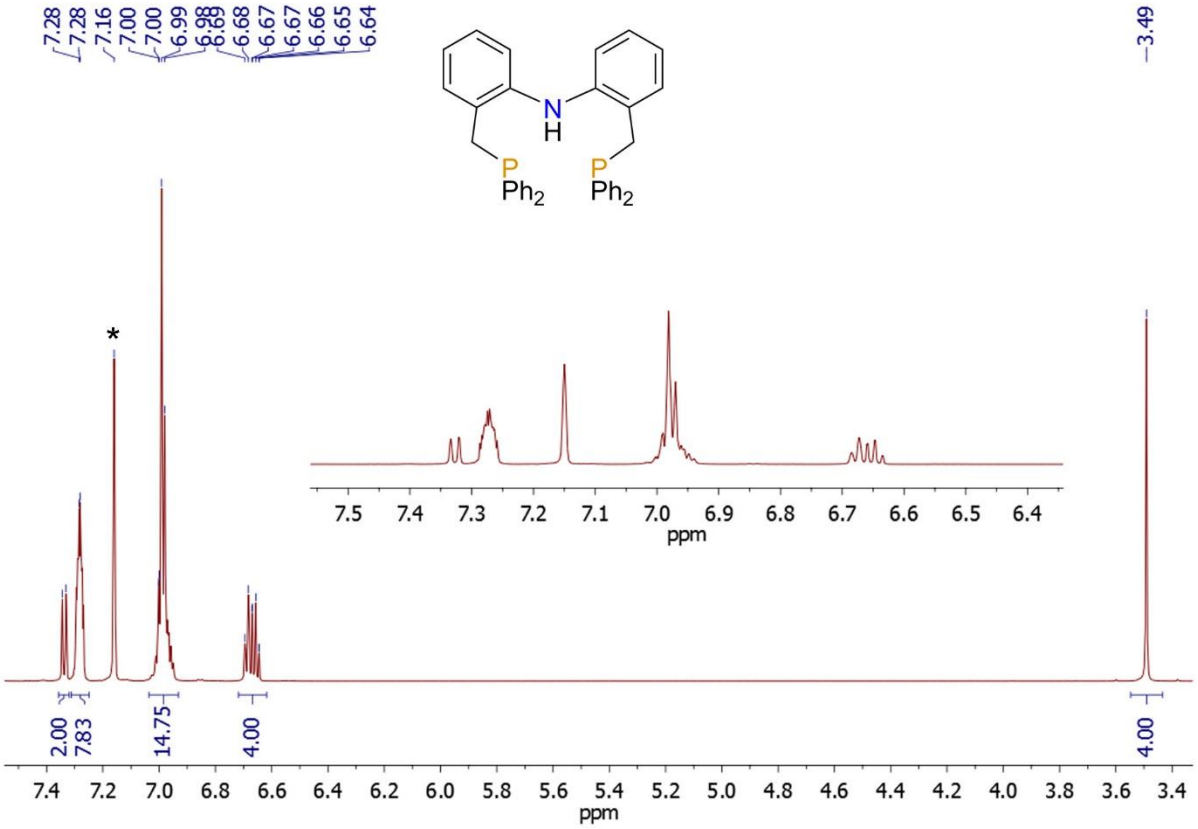


Fig. S8: $^{1}H$ NMR (600 MHz, $C_6D_6$) of [**B**]H (residual proton signals of $C_6D_6$ are labeled with ∗).

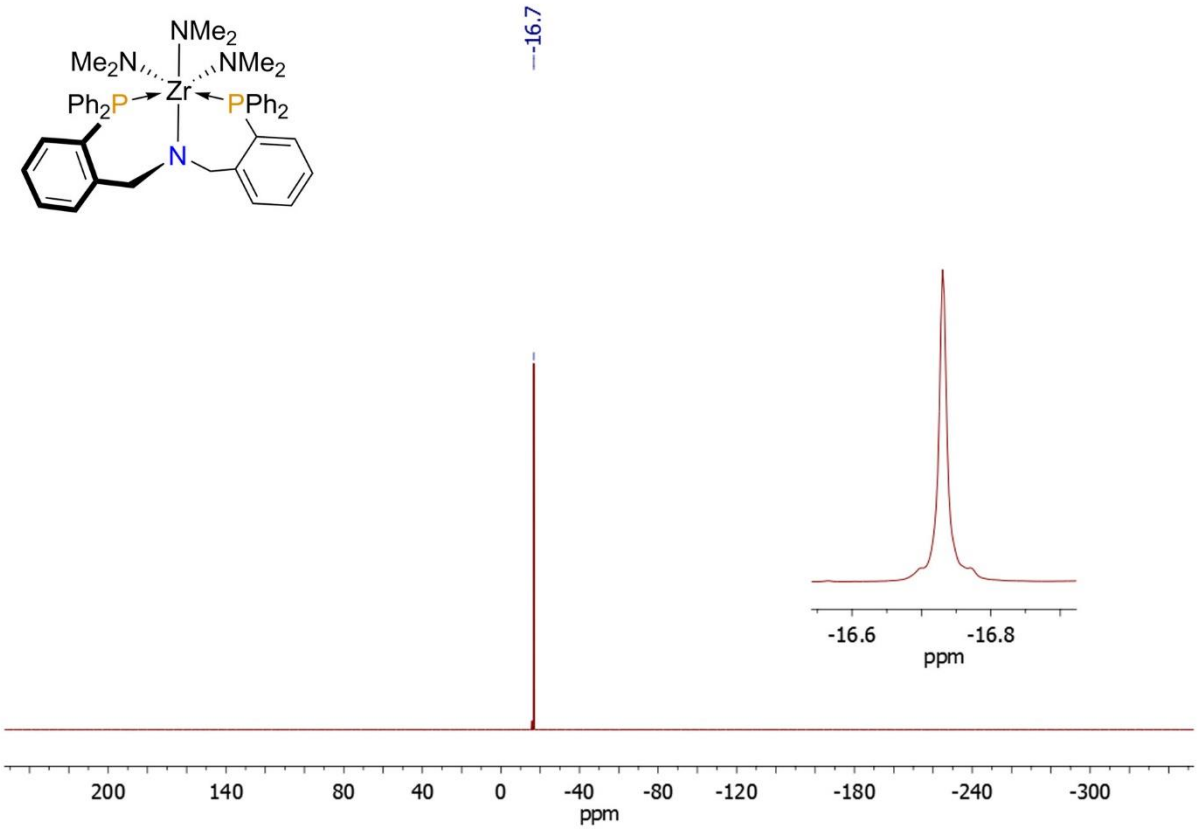


Fig. S9: $^{31}P\{^{1}H\}$ NMR (243 MHz, $C_6D_6$) of $^{[A]}$**1-Zr**.

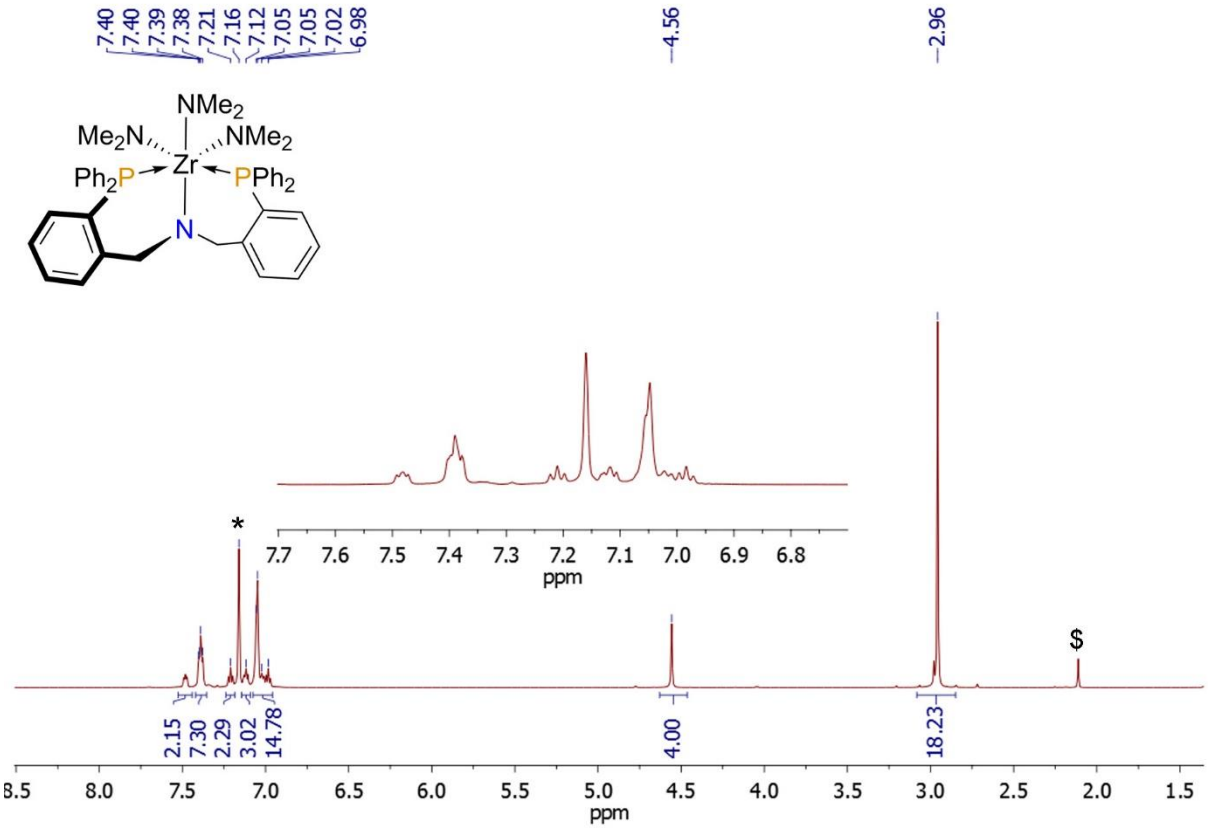


Fig. S10: $^{1}H$ NMR (600 MHz, $C_6D_6$) of $^{[A]}$**1-Zr** (residual toluene signals are labeled with §, residual proton signal of $C_6D_6$ is labeled with ∗).

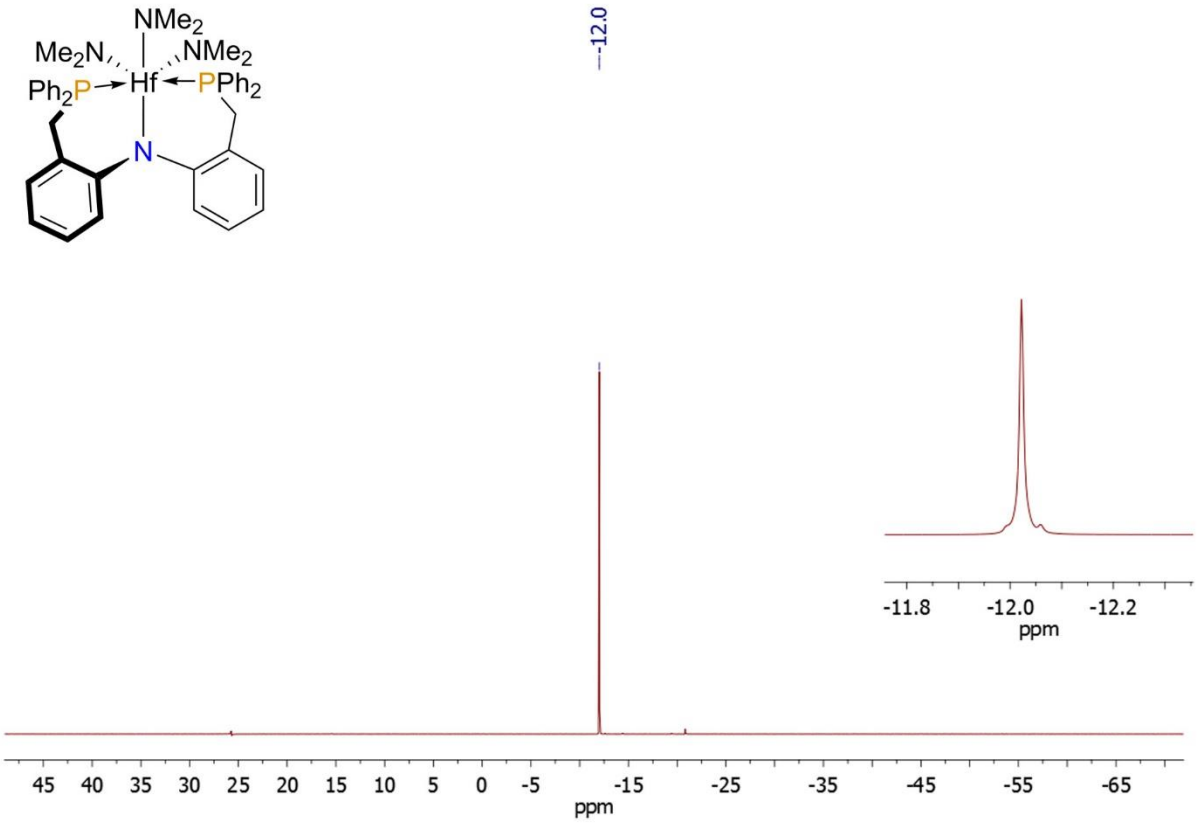


Fig. S11: $^{31}P\{^{1}H\}$ NMR (243 MHz, $C_6D_6$) of $^{[B]}$**1-Hf**.

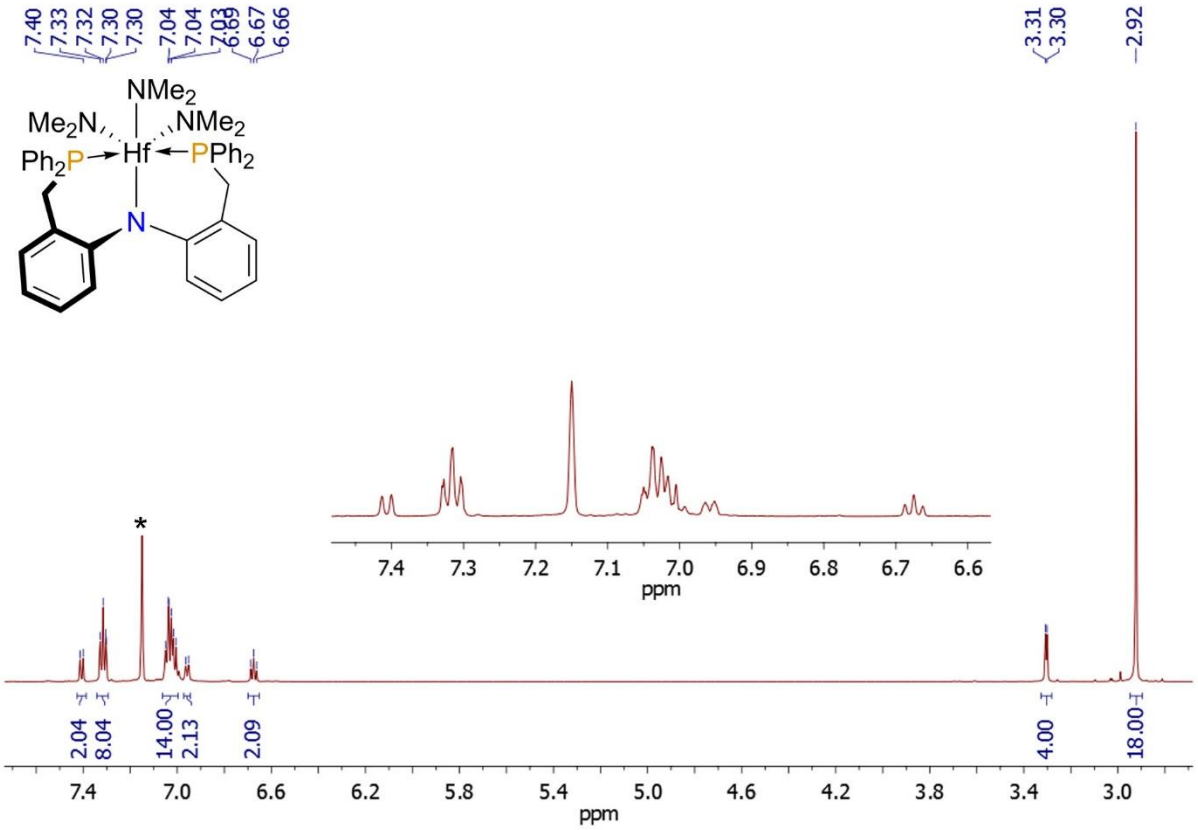


Fig. S12: $^{1}H$ NMR (600 MHz, $C_6D_6$) of $^{[B]}$**1-Hf** (residual proton signal of $C_6D_6$ is labeled with ∗).

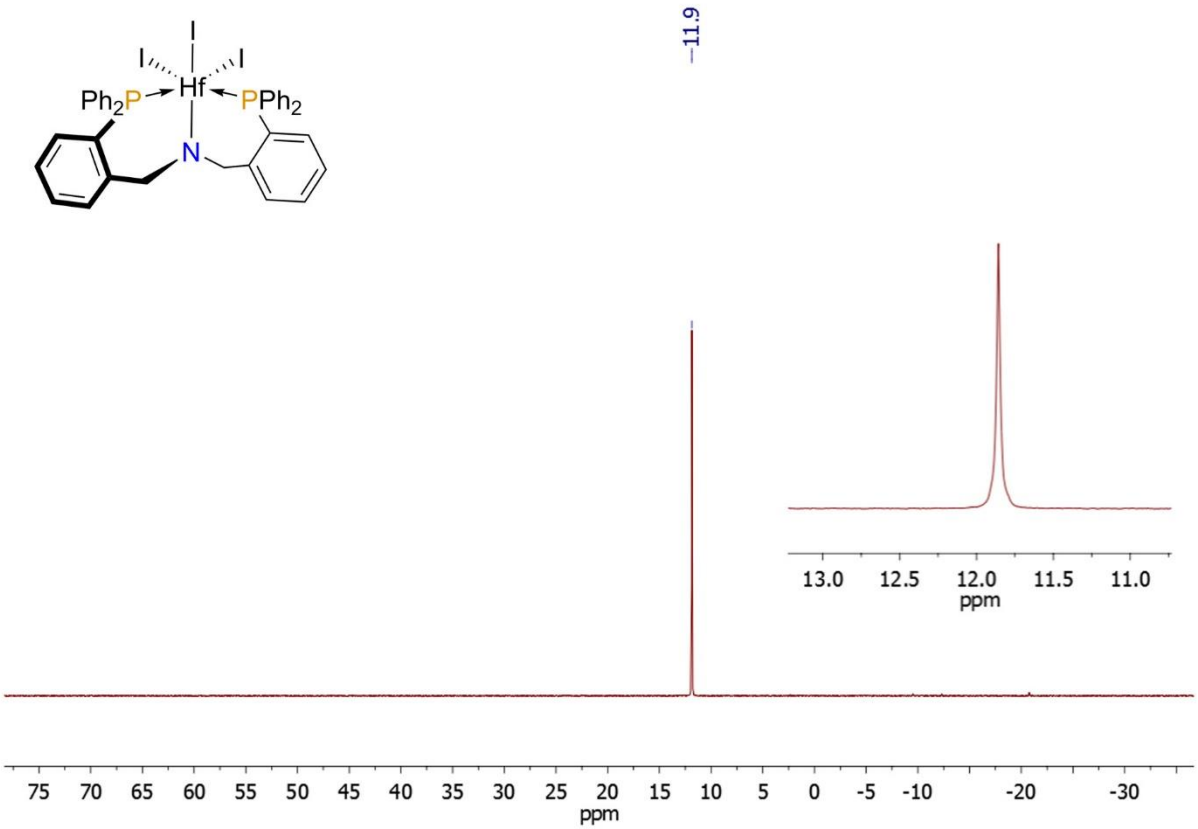


Fig. S13: $^{31}P\{^{1}H\}$ NMR (162 MHz, $CD_2Cl_2$) of $^{[A]}$**2-Hf**.

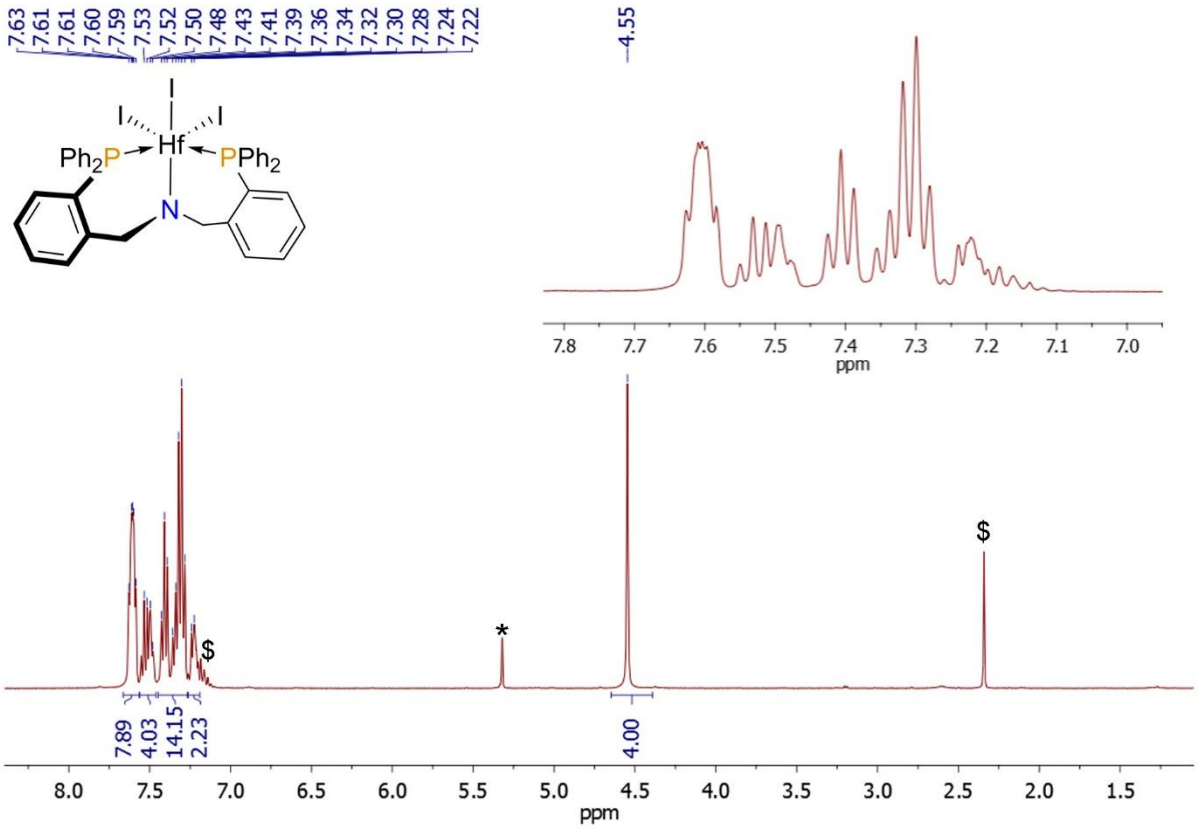


Fig. S14: $^{1}H$ NMR (400 MHz, $CD_2Cl_2$) of $^{[A]}$**2-Hf** (residual proton signal of $CD_2Cl_2$ is labeled with ∗, residual toluene signals are labeled with $).

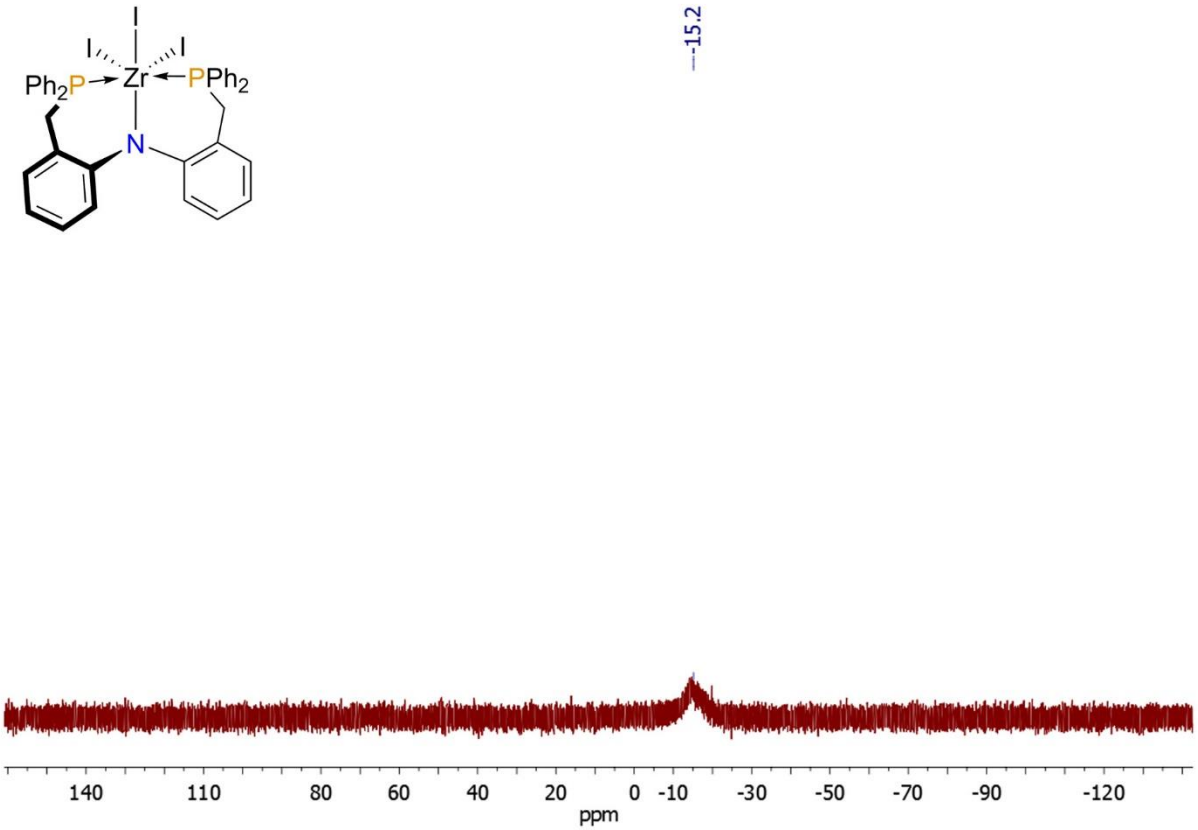


Fig. S15: $^{31}P\{^{1}H\}$ NMR (243 MHz $CD_2Cl_2$) of $^{[B]}$**2-Zr**.

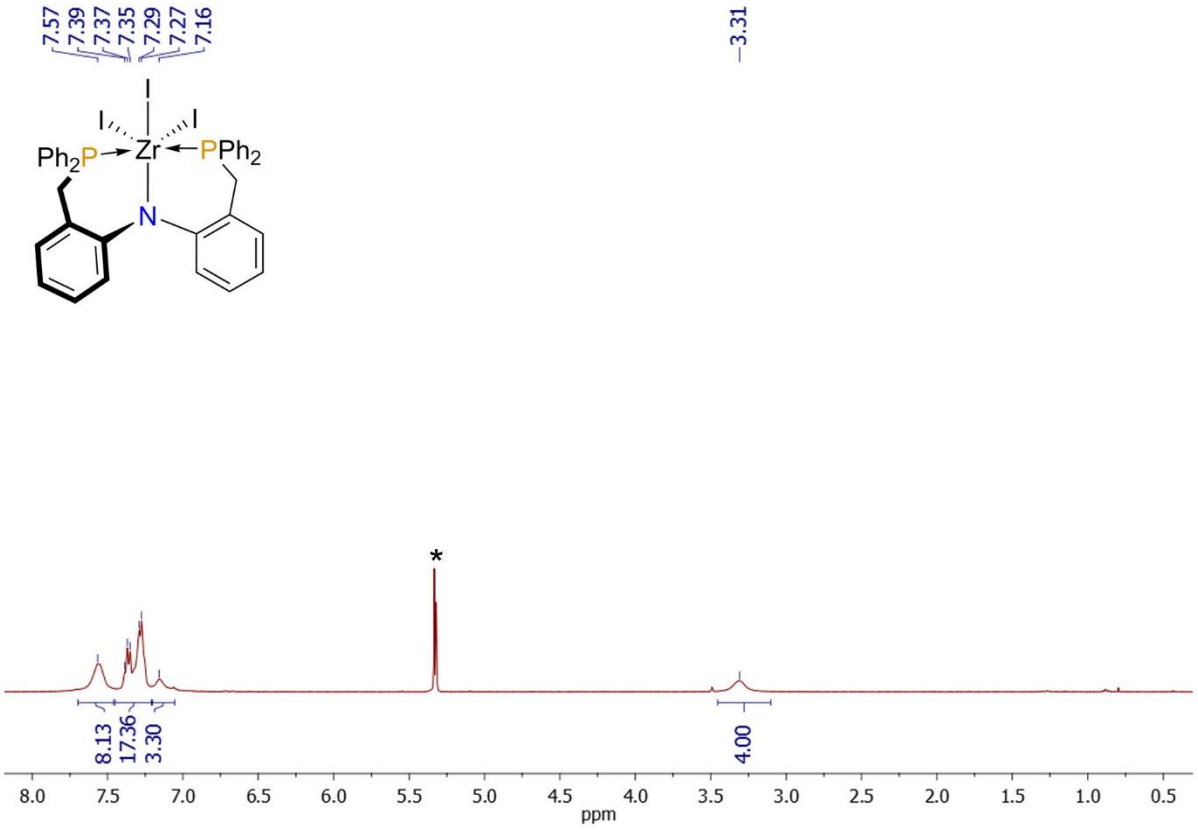


Fig. S16: $^{1}H$ NMR (600 MHz, $CD_2Cl_2$) of $^{[B]}$**2-Zr** (overlapping signals of residual $CH_2Cl_2$ and residual proton signals of $CD_2Cl_2$ are labeled with ∗).

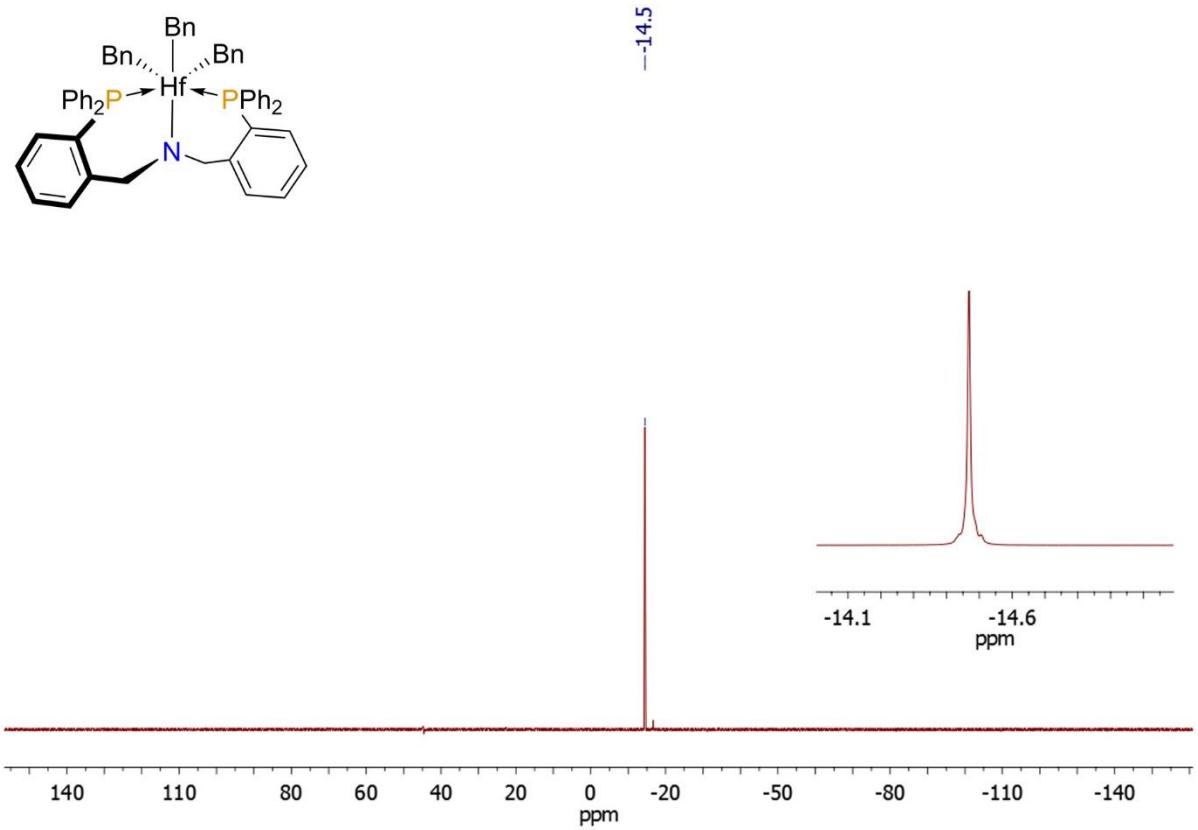


Fig. S17: $^{31}P\{^{1}H\}$ NMR (243 MHz, $C_6D_6$) of $^{[A]}$**3-Hf**.

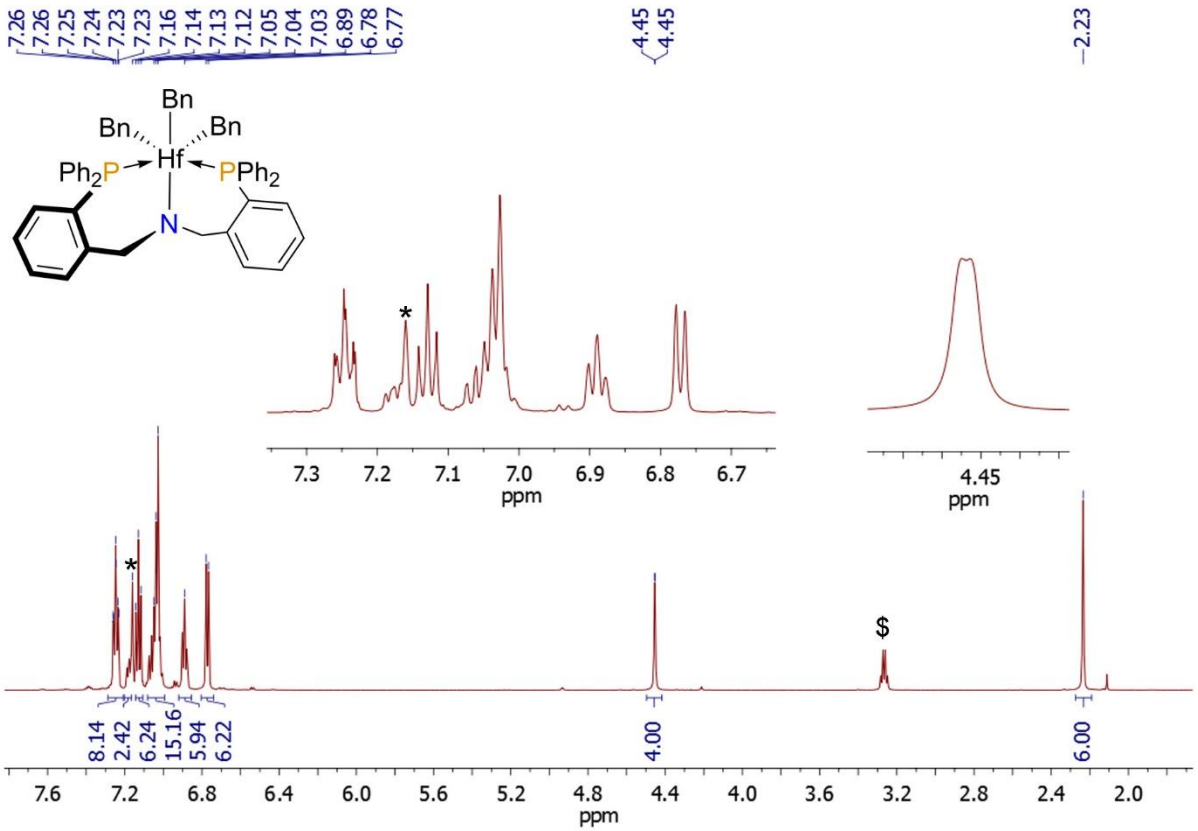


Fig. S18: $^{1}H$ NMR (600 MHz, $C_6D_6$) of $^{[A]}$**3-Hf** (α-protons of residual $Et_2O$ are labeled with $, the corresponding β-protons were detected at 1.73 ppm; residual proton signal of $C_6D_6$ is labeled with ∗).

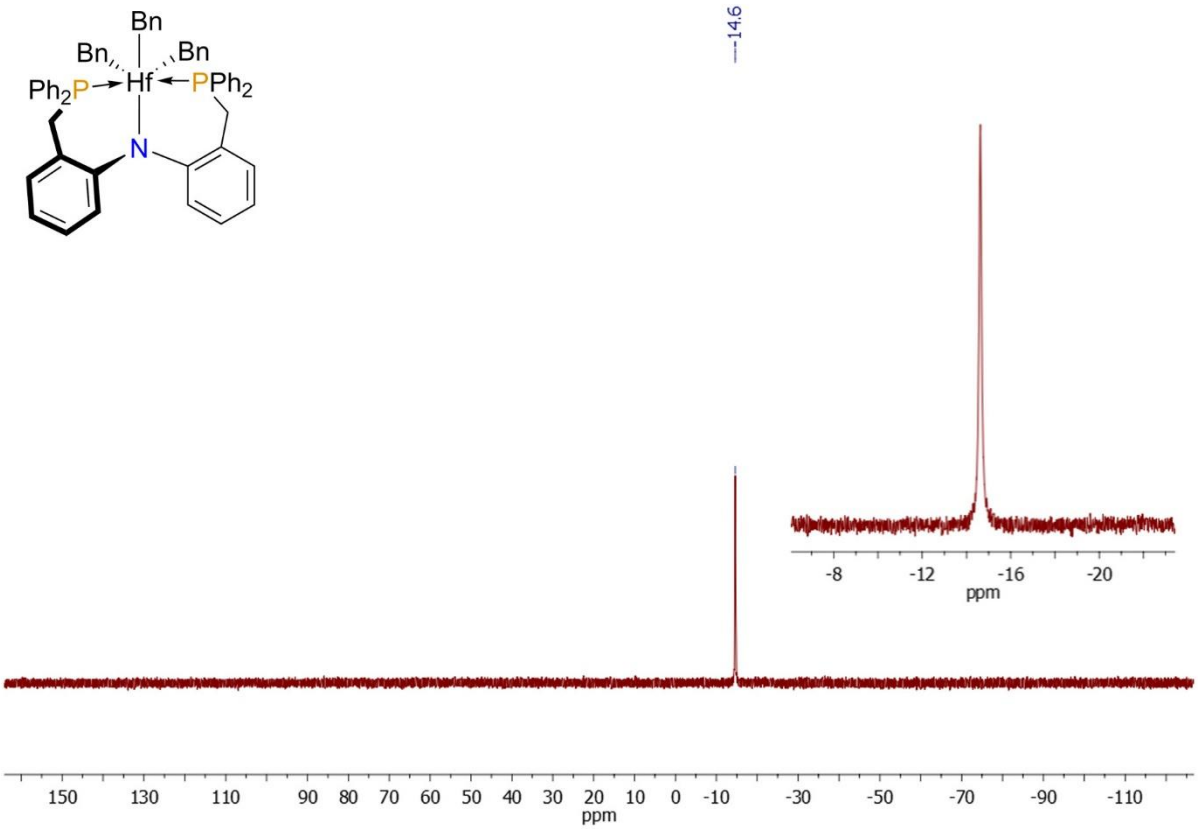


Fig. S19: $^{31}P\{^{1}H\}$ NMR (243 MHz, $C_6D_6$) of $^{[B]}$**3-Hf**.

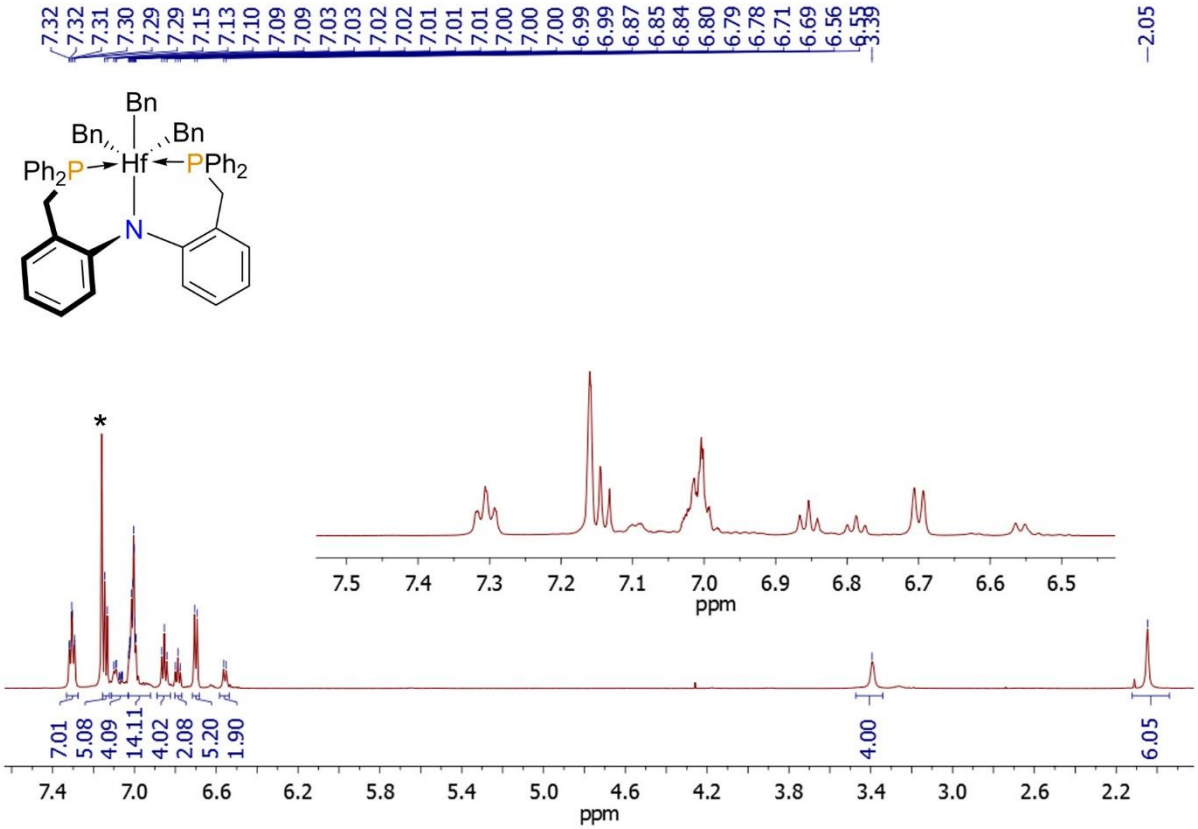


Fig. S20: $^{1}H$ NMR (600 MHz, $C_6D_6$) of $^{[B]}$**3-Hf** (residual proton signal of $C_6D_6$ is labeled with ∗).

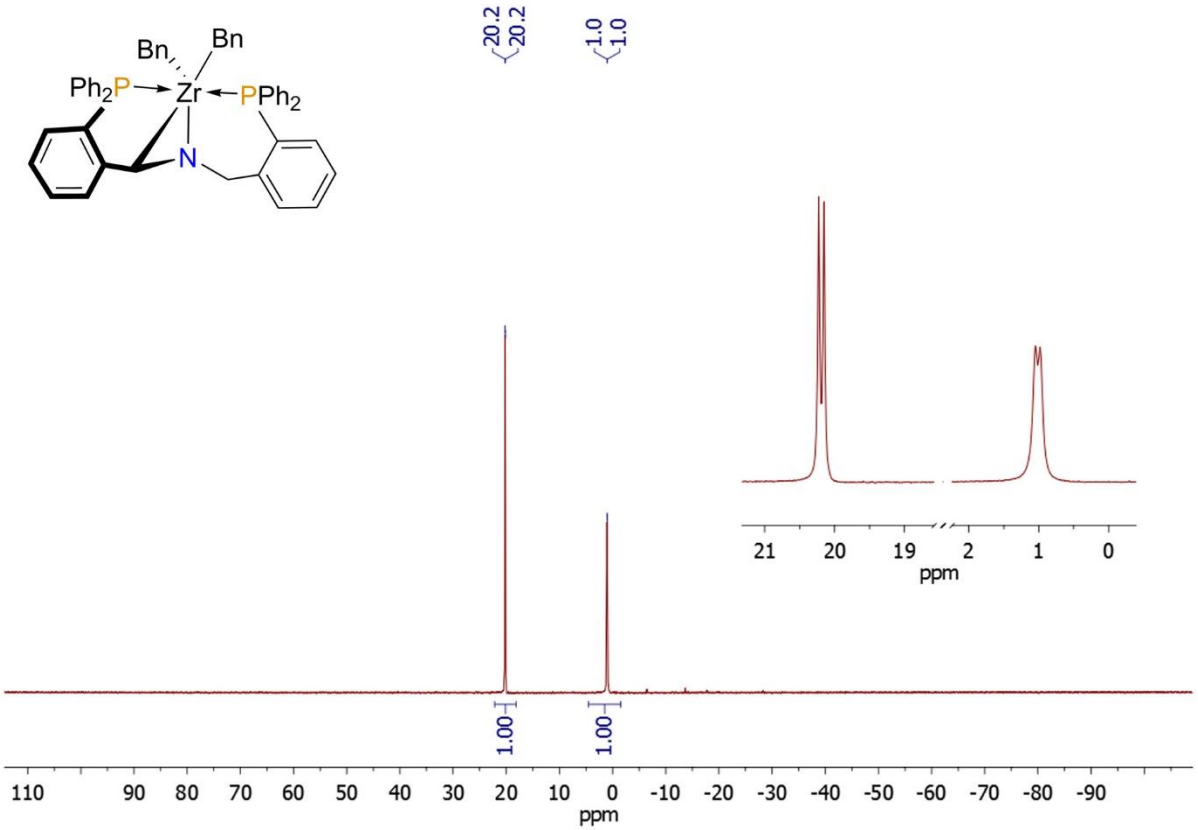


Fig. S21: $^{31}P\{^{1}H\}$ NMR (243 MHz, $C_6D_6$) of $^{[A]}$**4-Zr**.

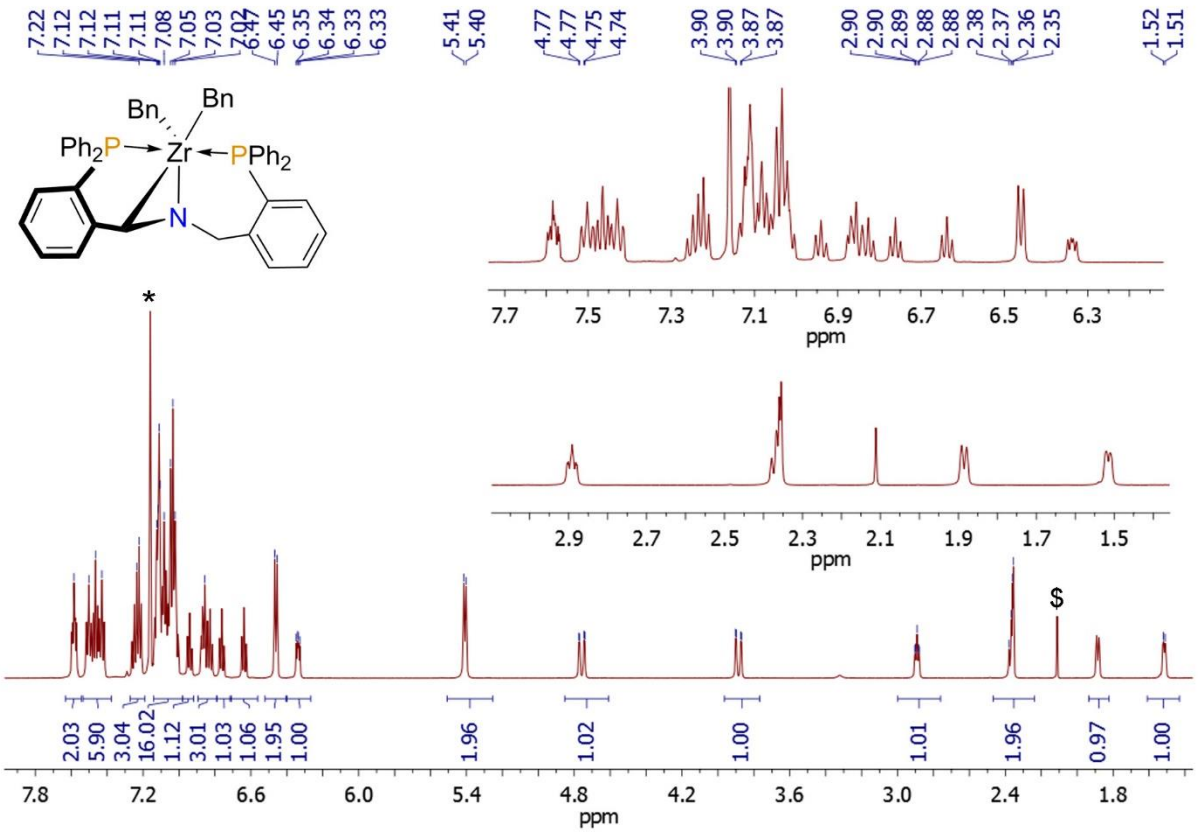


Fig. S22: $^{1}H$ NMR (600 MHz, $C_6D_6$) of $^{[A]}$**4-Zr** (residual toluene signal is labeled with $, residual proton signal of $C_6D_6$ is labeled with ∗).

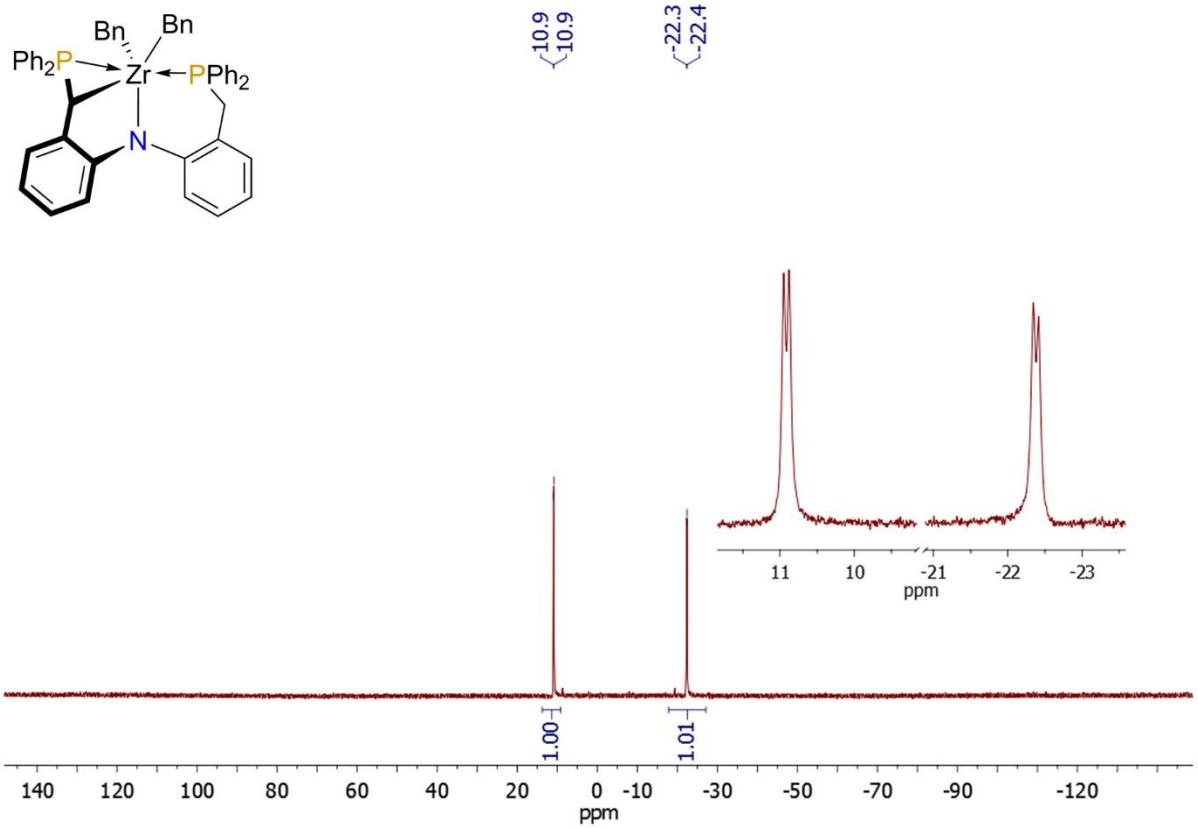


Fig. S23: $^{31}P\{^{1}H\}$ NMR (243 MHz, $C_6D_6$) of $^{[B]}$**4-Zr**.

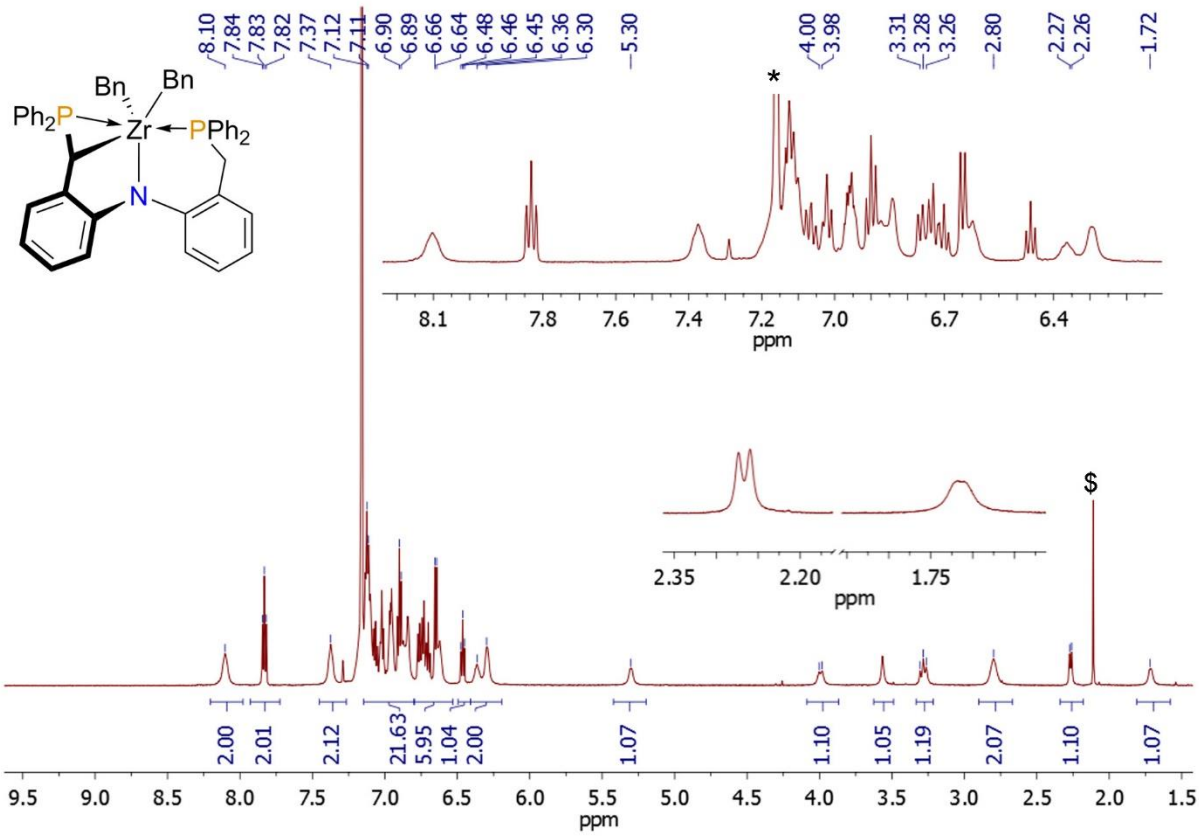


Fig. S24: $^{1}H$ NMR (600 MHz, $C_6D_6$) of $^{[B]}$**4-Zr** (residual toluene signals are labeled with §; residual proton signal of $C_6D_6$ is labeled with ∗).

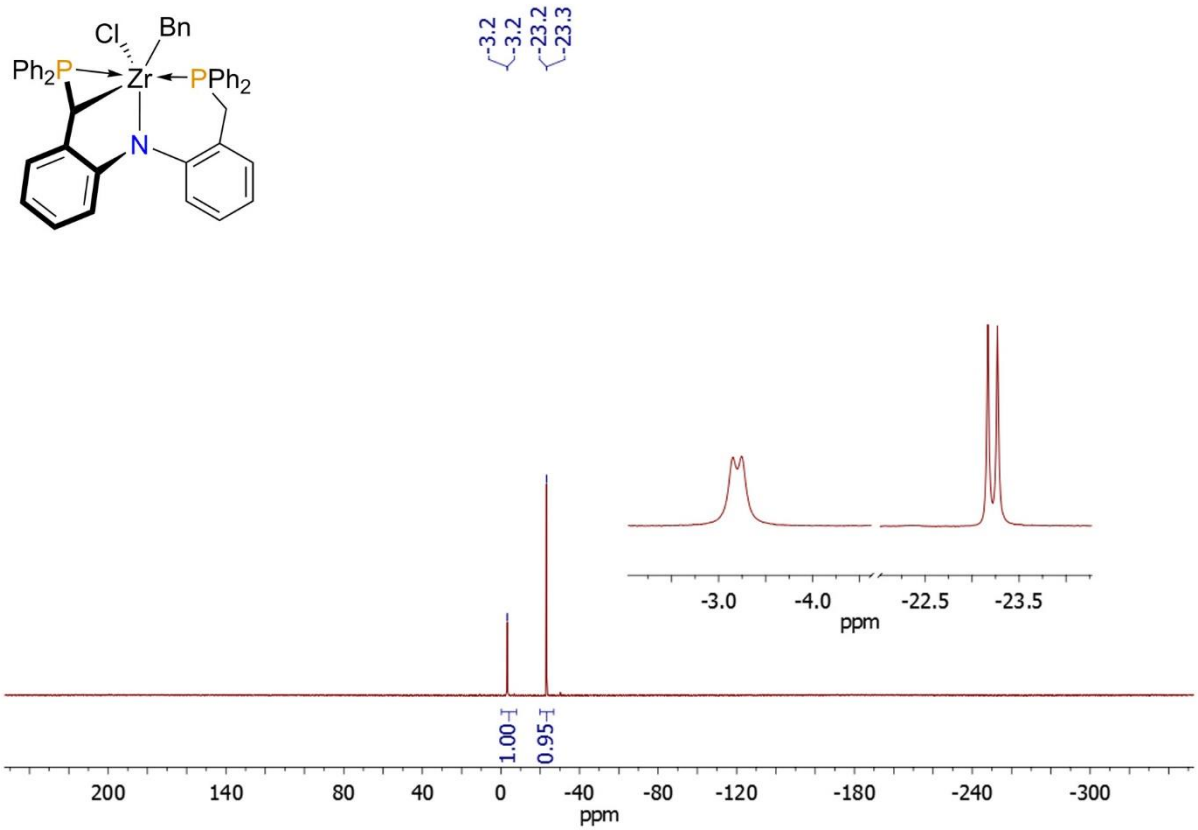


Fig. S25: $^{31}P\{^{1}H\}$ NMR (243 MHz, $C_6D_6$) of $^{[B]}$**5-Zr**.

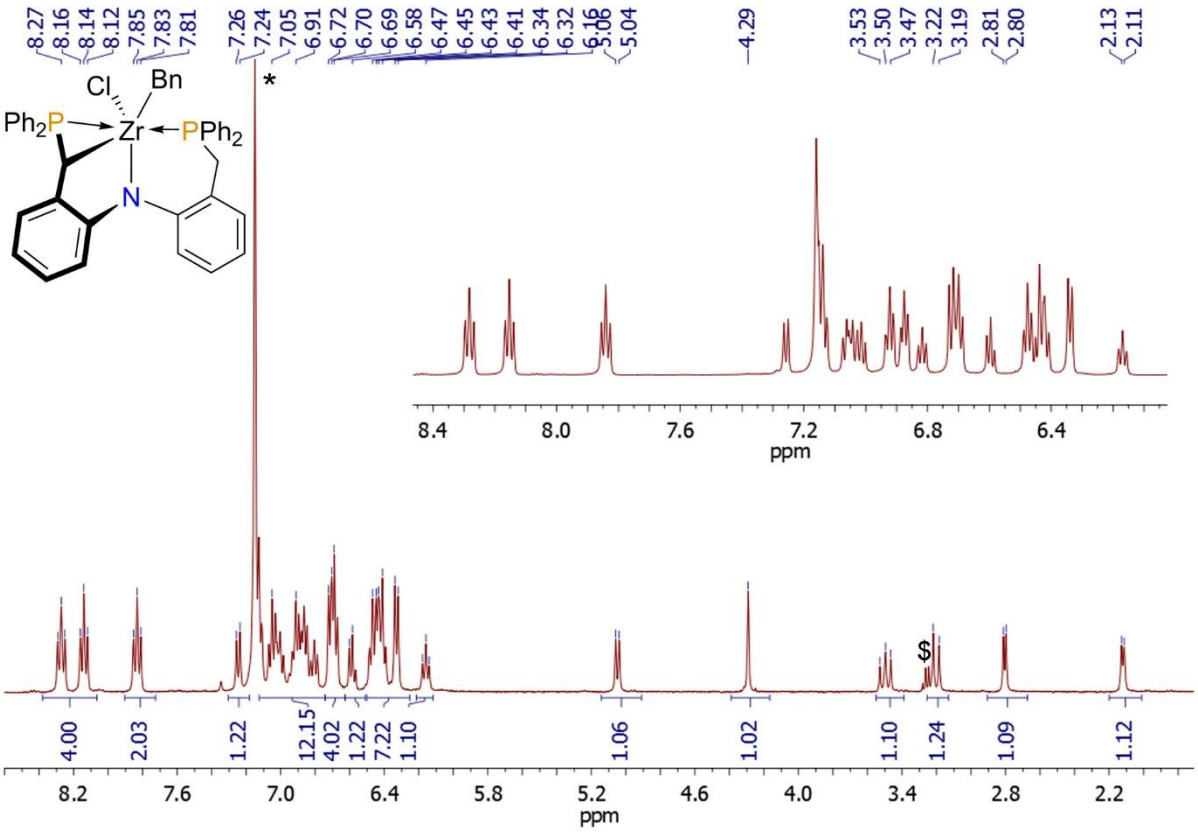


Fig. S26: $^{1}H$ NMR (600 MHz, $C_6D_6$) of $^{[B]}$**5-Zr** (residual $\alpha$-$Et_2O$ protons are labeled with $; residual proton signal of $C_6D_6$ is labeled with ∗).

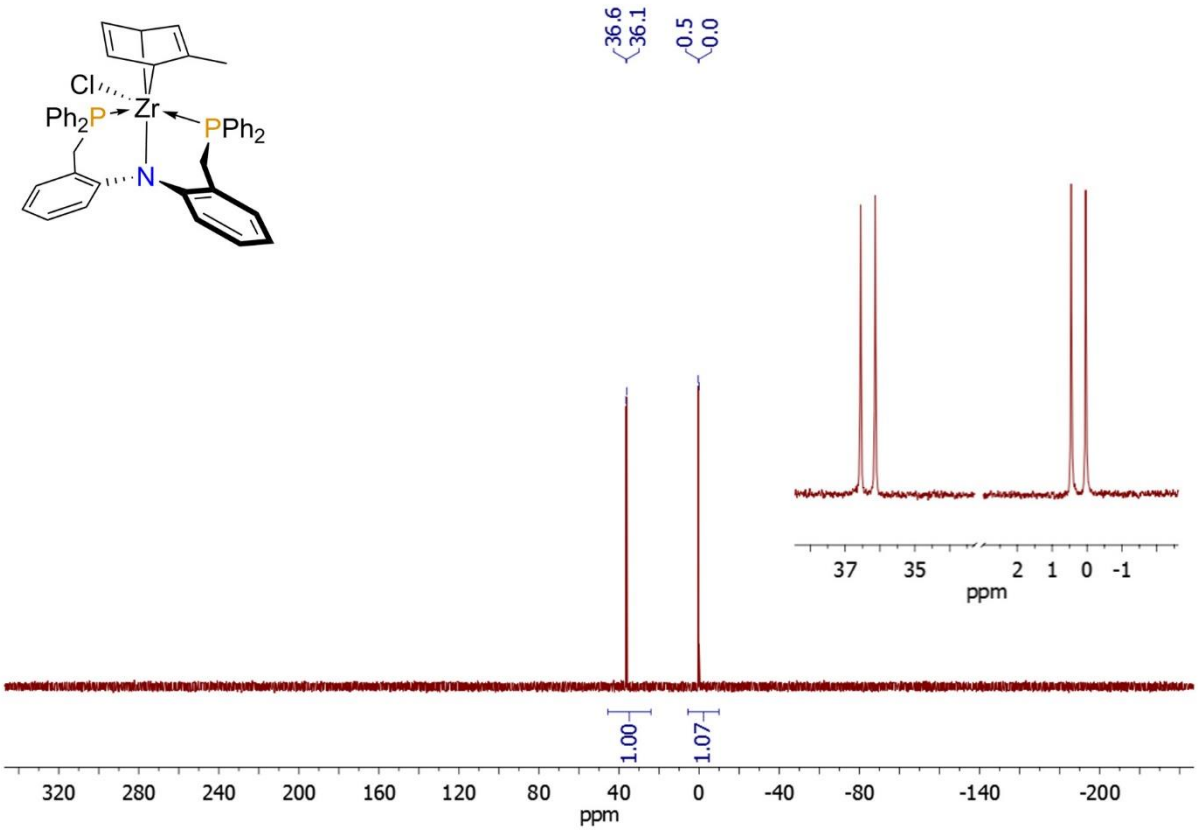


Fig. S27: $^{31}P\{^{1}H\}$ NMR (243 MHz, tol-$d_8$, −40 °C) of $^{[B]}$**6-Zr**.

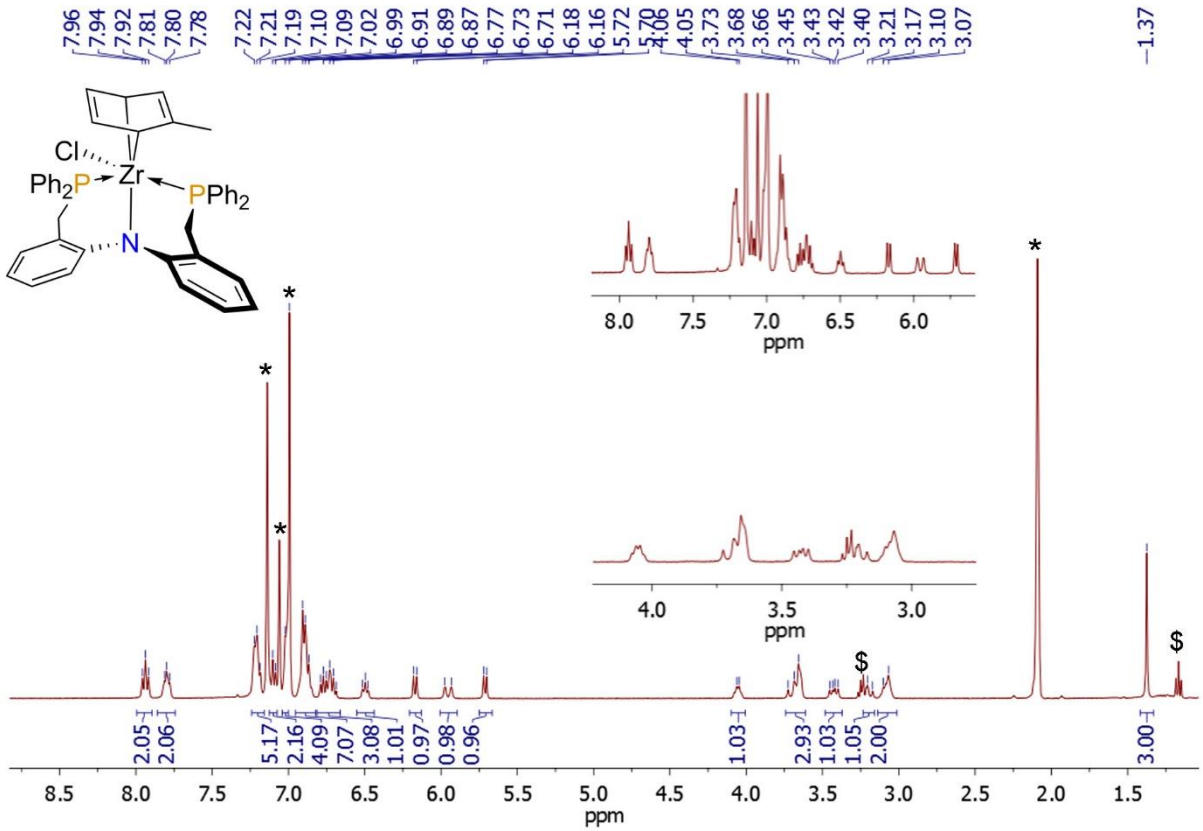


Fig. S28: $^{1}H$ NMR (600 MHz, tol-$d_8$, −40 °C) of $^{[B]}$**6-Zr** (residual proton signals of tol-$d_8$ are labeled with ∗, residual $Et_2O$ signals are labeled with $).

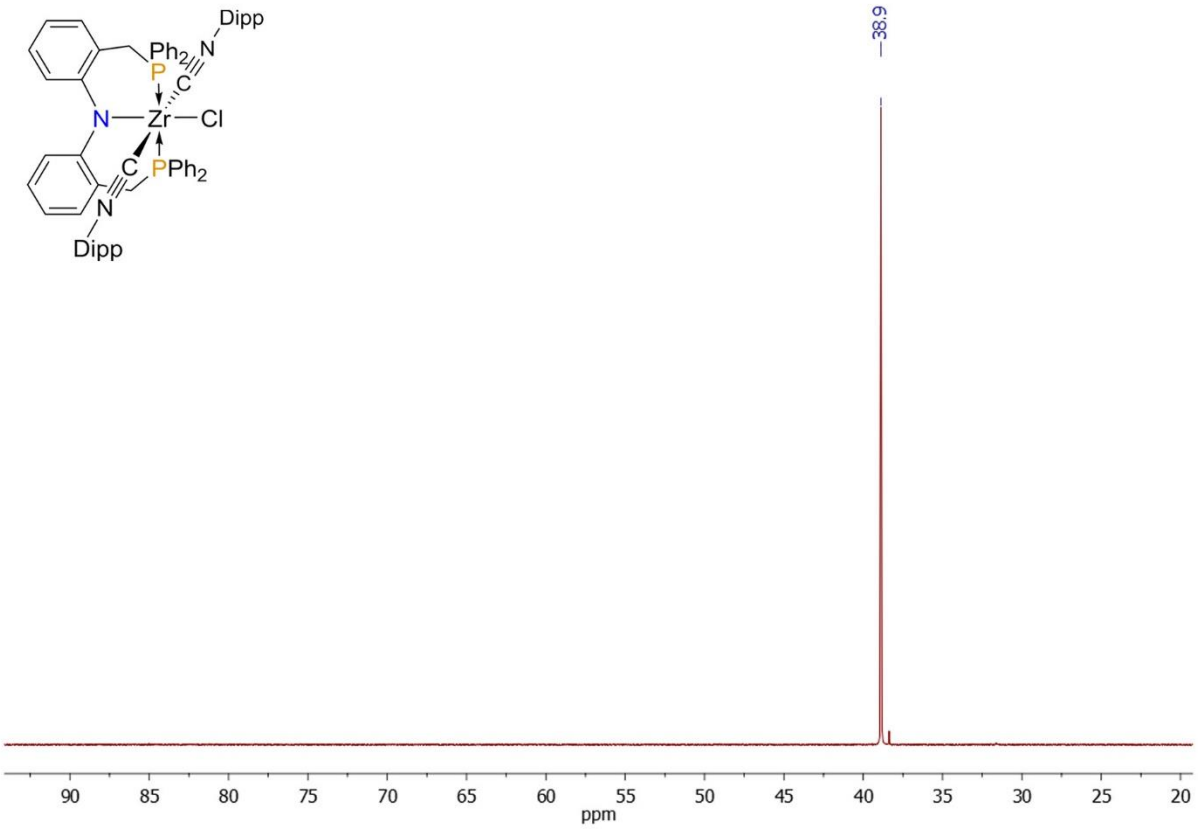


Fig. S29: $^{31}P\{^{1}H\}$ NMR (243 MHz, $C_6D_6$) of $^{[B]}$**7-Zr**.

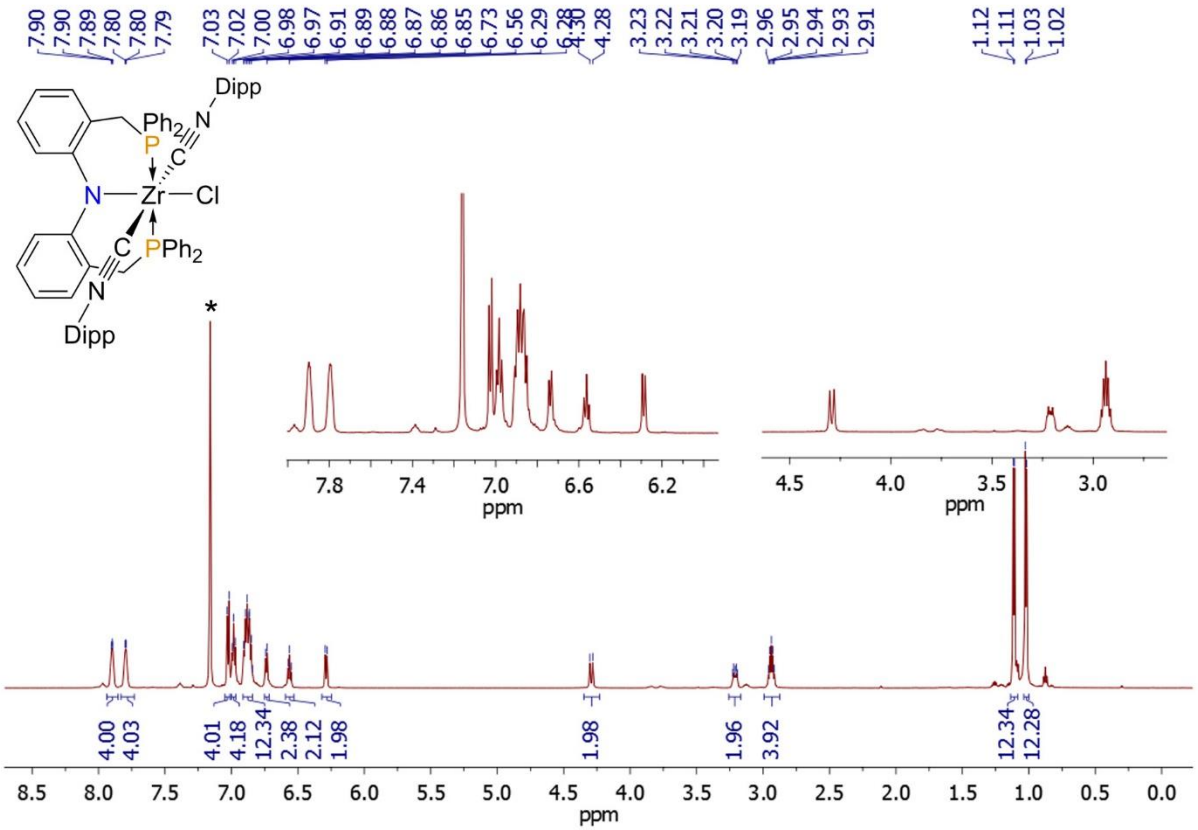


Fig. S30: $^{1}H$ NMR (600 MHz, $C_6D_6$) of $^{[B]}$**7-Zr** (residual proton signal of $C_6D_6$ is labeled with ∗).

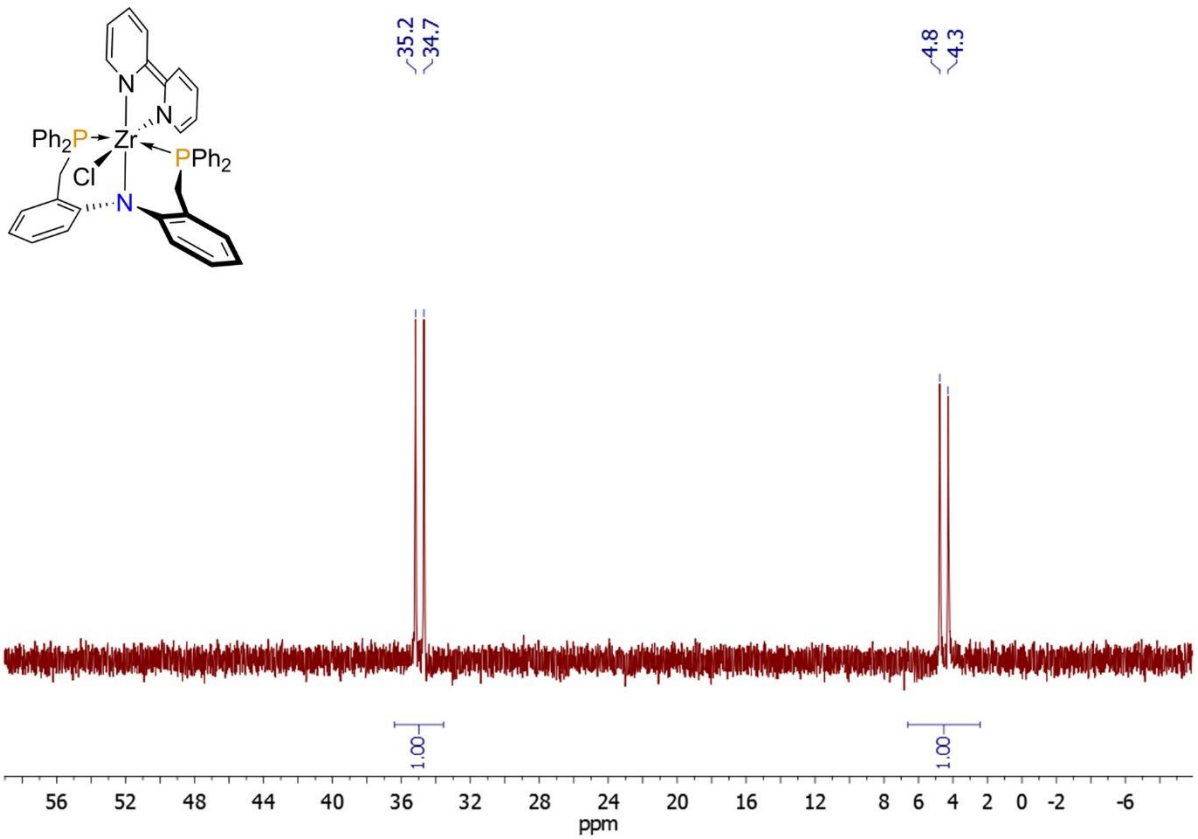


Fig. S31: $^{31}P\{^{1}H\}$ NMR (243 MHz, $C_6D_6$) of $^{[B]}$**8-Zr**.

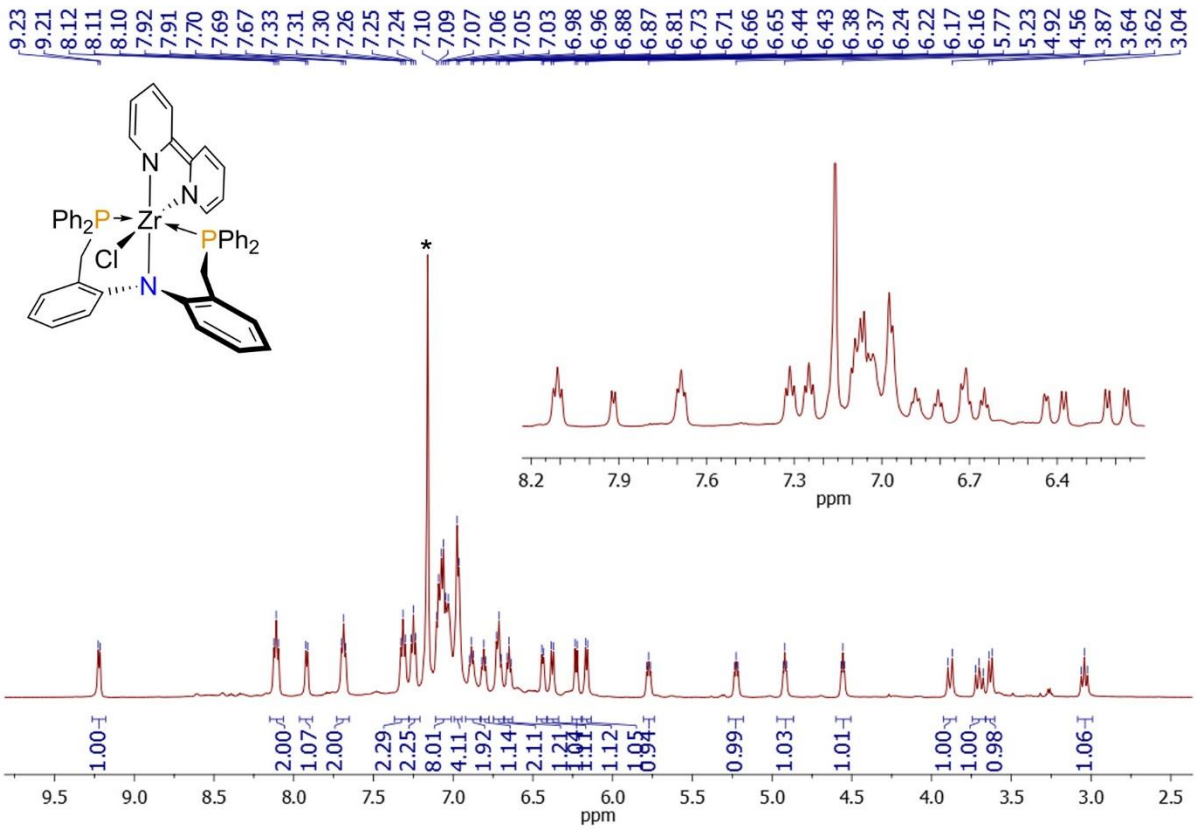


Fig. S32: $^{1}H$ NMR (600 MHz, $C_6D_6$) of $^{[B]}$**8-Zr** (residual proton signal of $C_6D_6$ is labeled with ∗).

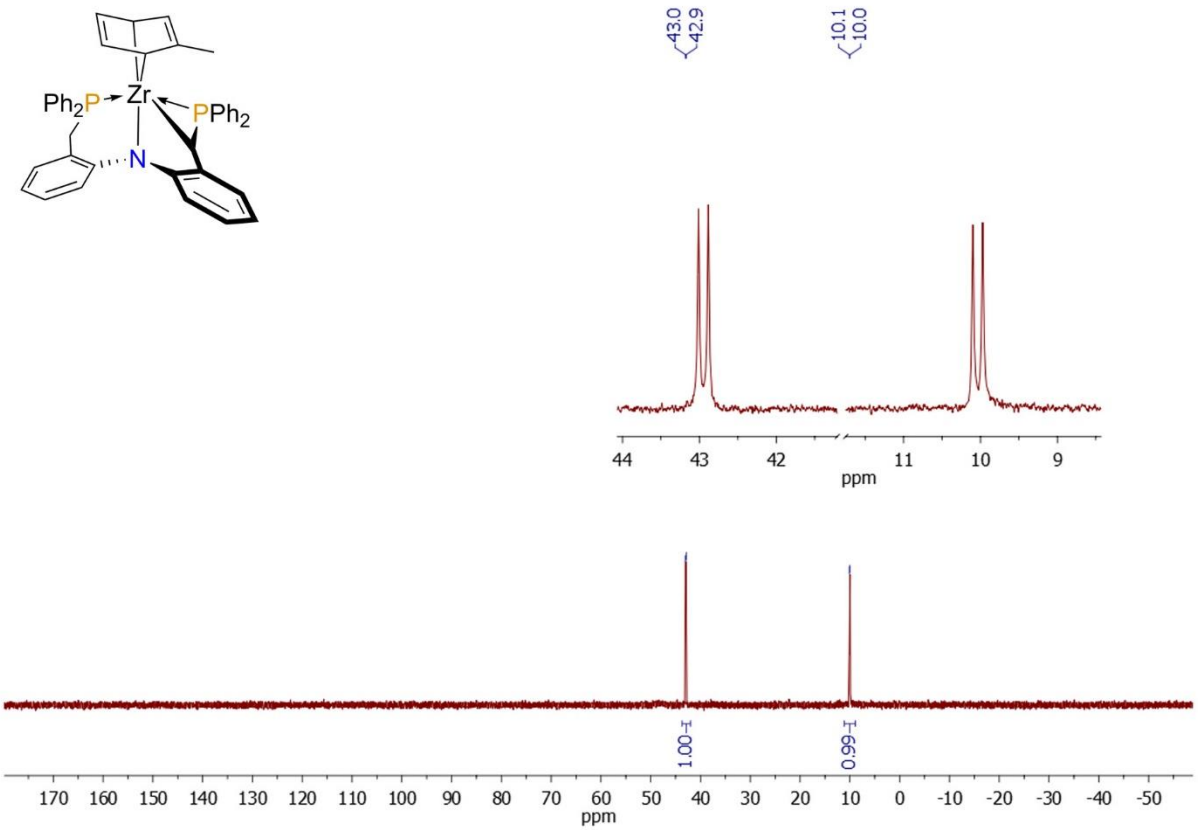


Fig. S33: $^{31}P\{^{1}H\}$ NMR (243 MHz, $C_6D_6$) of $^{[B]}$**9-Zr**.

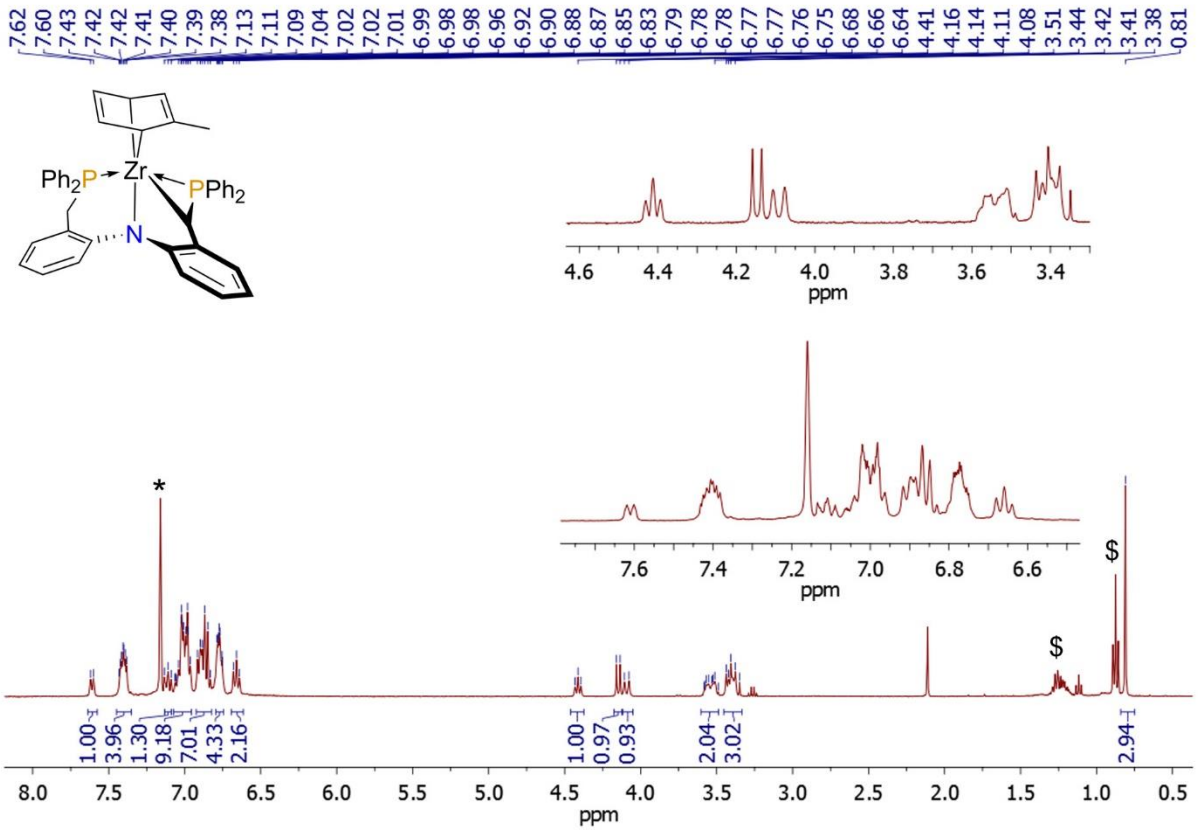


Fig. S34: $^{1}H$ NMR (600 MHz, $C_6D_6$) of $^{[B]}$**9-Zr** (residual proton signal of $C_6D_6$ is labeled with ∗, residual pentane signals are labeled with $).

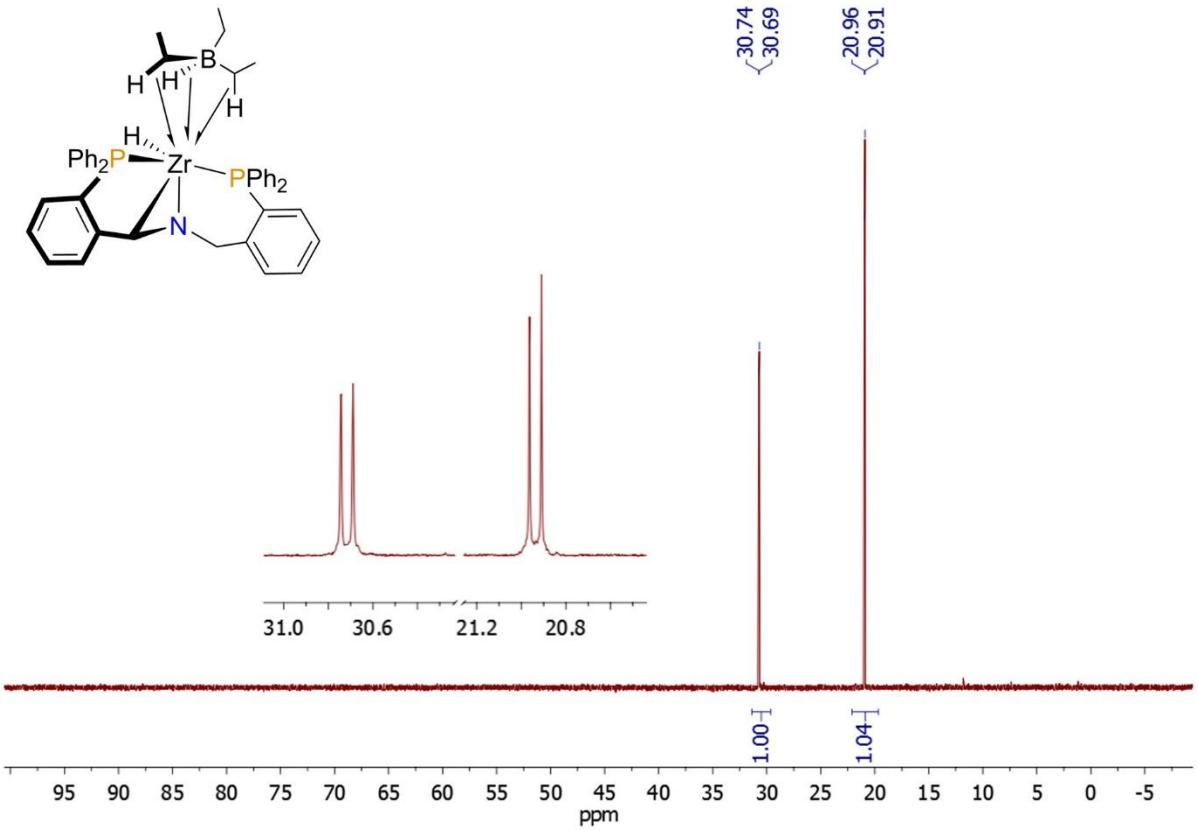


Fig. S35: $^{31}P\{^{1}H\}$ NMR (243 MHz, $C_6D_6$) of $^{[A]}$**10-Zr**.

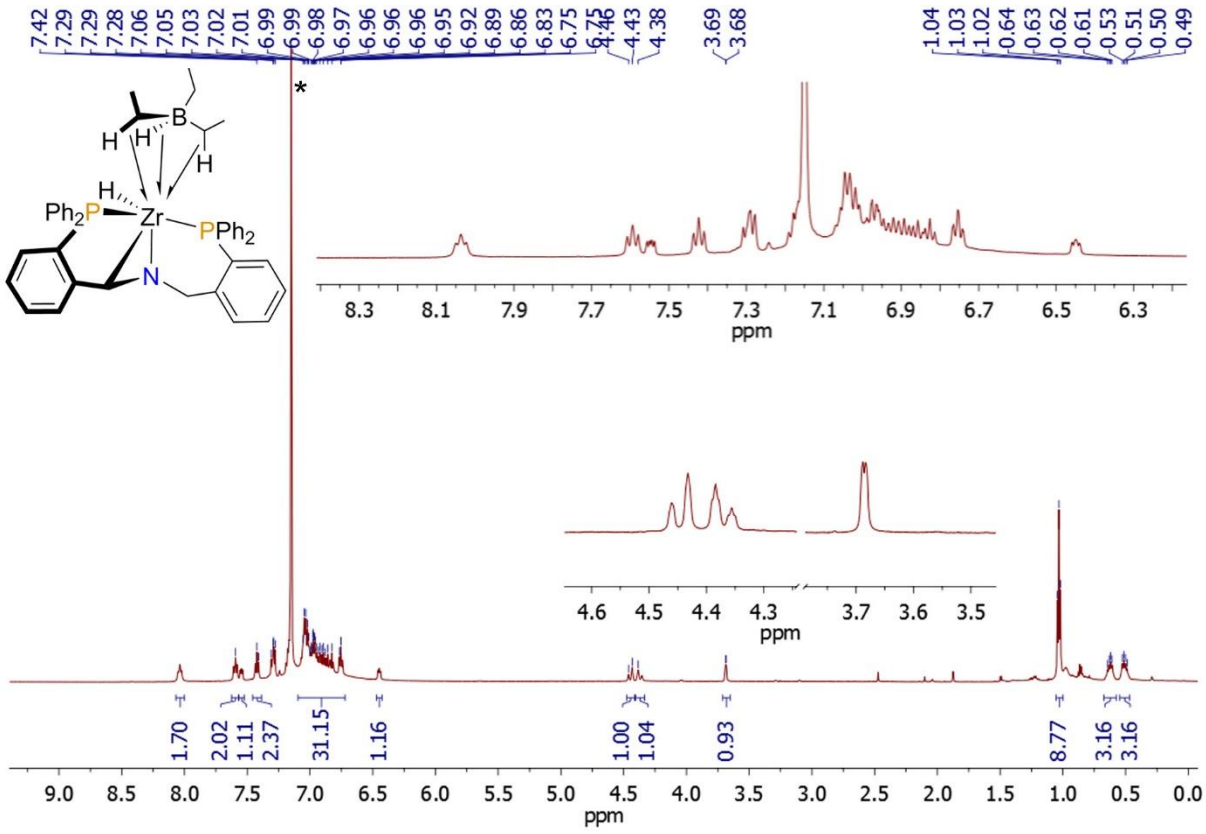


Fig. S36: $^{1}H$ NMR (600 MHz, $C_6D_6$) of $^{[A]}$**10-Zr** (residual proton signal of $C_6D_6$ is labeled with ∗, manually picked crystals were used to record the spectrum of this highly sensitive compound; unknown impurities in the aliphatic region are clearly visible, despite the use of rigorously dried $C_6D_6$).

## 4) Selected IR und UV-Vis Spectra

IR spectra were acquired on a Varian 3100 FT-IR spectrometer (Excalibur series) of a nujol mull of the compounds at room temperature using a NaCl cell. UV/Vis absorption spectra were acquired on a Cary 5000 UV/Vis/NIR spectrometer.

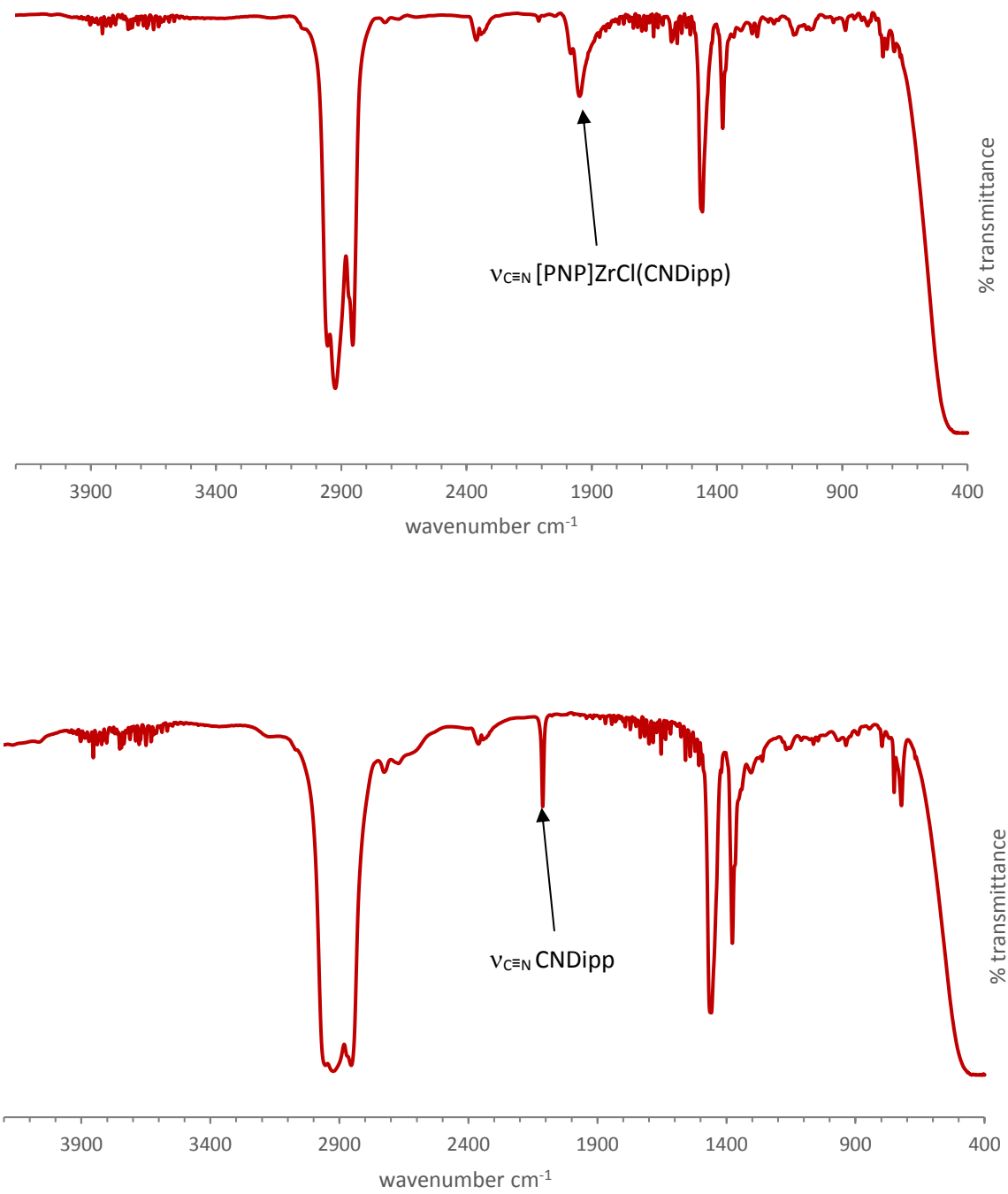


Fig. S37: IR spectra (nujol mull) of [**B**]ZrCl(CNDipp)$_2$ (top) and CNDipp (bottom).

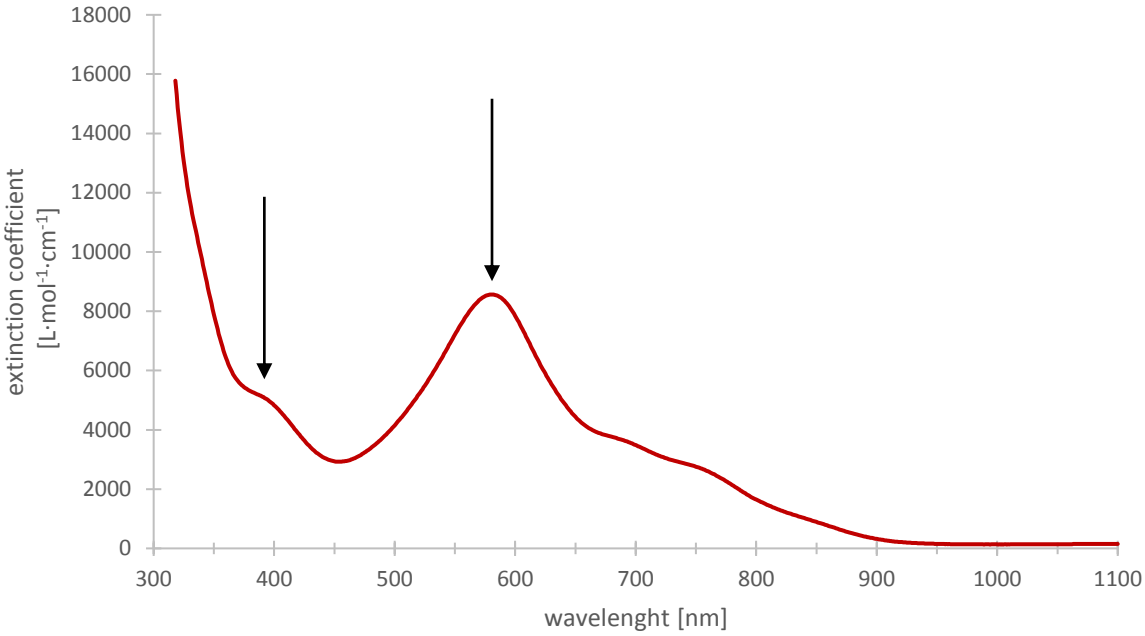


Fig. S38: UV-Vis spectrum of [**B**]ZrCl(bipy) ([B]**8-Zr**) recorded in toluene at room temperature.

## 5) Details on DFT Calculations

DFT calculations were performed with the Gaussian 09 program suite(G09RevB.01)[1] using the hybrid functional B3PW91.[2] Effective core potentials were used to describe Zr and I (Stuttgart-Dresden basis set augmented with a set of f-functions).[3] Carbons and nitrogens have been described with 6-31G(d) basis set, protons with the 6-31G basis set and phosphorus atoms were described with 6-311+G(d,p) including polarization functions.[4] Geometry optimizations were carried out without symmetry restrictions and the stationary point were identified as minima by analytical frequency analysis. Natural bond orbital analysis was carried out with the NBO-3.1 program[5] implemented in Gaussian 09.

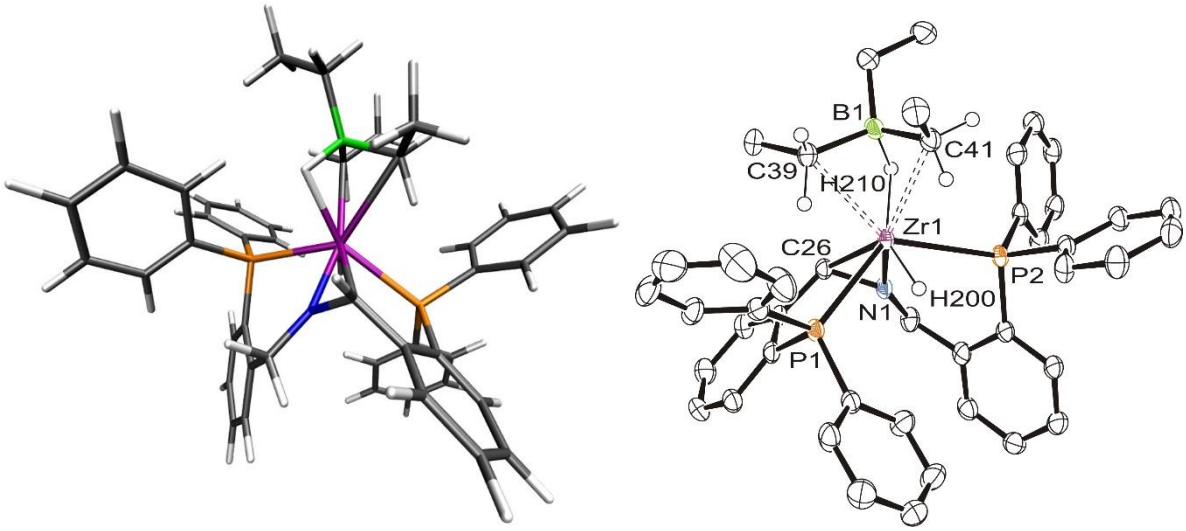


Fig. S39: DFT-optimised (left) and crystallographically determined structure (right) of [A]**10-Zr**.

*DFT-optimised coordinates of* $^{[A]}$***10-Zr***

Charge = 0 Multiplicity = 1

| | | | |
|---|---|---|---|
| C | -3.79810 | -1.51813 | -4.08018 |
| C | -4.63436 | -1.86363 | -3.01694 |
| C | 5.56670 | -0.78098 | -2.51731 |
| C | 0.84376 | -1.85269 | -2.14776 |
| C | 4.78198 | 1.49241 | -2.68761 |
| C | 1.34699 | -4.10150 | -1.16772 |
| C | 1.48012 | -2.71286 | -1.07793 |
| C | -3.04747 | -0.86750 | -1.48256 |
| C | 3.80714 | 1.22901 | -1.72633 |
| C | 2.64249 | 4.84986 | 0.06290 |
| C | 2.19941 | -2.17348 | 0.01148 |
| C | 2.60111 | -4.41793 | 0.86168 |
| C | 2.74677 | -3.03616 | 0.96973 |
| C | -1.82123 | -2.64646 | 1.45047 |
| C | -2.84425 | -1.70432 | 1.28011 |
| C | -2.03700 | -3.78646 | 2.2210 |
| C | 3.31632 | -0.09567 | 1.73224 |
| C | -5.58409 | 2.96376 | 1.50336 |
| C | -3.26907 | -3.99325 | 2.84098 |
| C | -4.28878 | -3.05685 | 2.68243 |
| C | -4.66467 | 2.42634 | 2.40574 |
| C | 4.56714 | 0.33883 | 4.20468 |
| H | -4.08975 | -1.75864 | -5.10023 |
| H | 6.41784 | 0.69254 | -3.84095 |
| H | -5.57802 | -2.37145 | -3.19861 |
| H | 0.13988 | -2.47264 | -2.72129 |
| H | 0.78568 | -4.51995 | -2.00064 |
| H | 4.84651 | 2.48400 | -3.12817 |
| H | -0.90571 | 4.75301 | -2.31656 |
| H | 1.35403 | 4.71984 | -1.65376 |
| H | -2.24168 | 3.62446 | -2.57783 |
| H | -4.90739 | -1.78233 | -0.88427 |
| H | 3.11601 | 2.01369 | -1.43341 |
| H | 0.60784 | 5.46497 | -0.26394 |
| H | -1.64371 | 2.26181 | -0.74142 |
| H | -0.85351 | -2.47694 | 0.98735 |
| H | -1.61759 | 3.85017 | -0.11016 |
| H | 3.29603 | -2.62320 | 1.81064 |
| H | -1.23472 | -4.50981 | 2.34215 |
| H | 0.28775 | 1.81808 | 1.74809 |
| H | 0.11285 | 4.84589 | 2.10561 |
| H | -1.25788 | 3.73406 | 2.13640 |
| H | -3.06233 | 1.02432 | 2.70213 |
| H | 1.50785 | -0.34964 | 2.87888 |
| H | 0.00254 | 3.61173 | 3.36886 |
| H | 5.05207 | 0.50902 | 5.16266 |
| B | 0.51008 | 3.23080 | -0.20237 |
| P | 2.42302 | -0.35160 | 0.14648 |
| Zr | -0.04275 | 0.77334 | -0.25638 |
| C | -2.57966 | -0.88953 | -3.84101 |
| C | 5.66212 | 0.48833 | -3.08662 |
| C | -2.1603 | -0.56898 | -2.53747 |
| C | -0.82696 | 0.05169 | -2.29411 |
| C | 4.59654 | -1.04524 | -1.55227 |
| C | -4.25352 | -1.53648 | -1.71805 |
| C | -1.20380 | 3.70259 | -2.23032 |
| C | 1.90173 | -4.95368 | -0.21555 |
| C | 3.70614 | -0.04111 | -1.14335 |
| C | 1.26160 | 4.62871 | -0.56201 |
| C | -1.04111 | 3.20741 | -0.79064 |
| C | -4.73306 | 1.50058 | -0.22506 |
| C | -5.61270 | 2.50177 | 0.18956 |
| C | -3.81346 | 0.95075 | 0.67547 |
| C | 0.60652 | 2.83714 | 1.40698 |
| C | 4.68709 | 0.18530 | 1.79497 |
| C | -4.08077 | -1.91951 | 1.90281 |
| C | -3.78013 | 1.43335 | 1.99407 |
| C | -0.17707 | 3.80746 | 2.30370 |
| C | 5.30627 | 0.40425 | 3.02553 |
| C | 2.57584 | -0.14815 | 2.92405 |
| C | 3.20132 | 0.05935 | 4.15072 |
| H | -1.92145 | -0.65044 | -4.67440 |
| H | 6.24852 | -1.57019 | -2.82443 |
| H | 1.61677 | -1.51825 | -2.86525 |
| H | -0.44562 | 0.54182 | -3.20465 |
| H | -0.57978 | 3.12421 | -2.92195 |
| H | 4.52964 | -2.03839 | -1.11663 |
| H | 1.77832 | -6.02937 | -0.31281 |
| H | 3.34062 | 4.04166 | -0.19214 |
| H | 3.09946 | 5.78983 | -0.27456 |
| H | 1.18167 | 2.33577 | -0.85703 |
| H | -4.76242 | 1.14578 | -1.25127 |
| H | 2.59265 | 4.89132 | 1.15786 |
| H | -6.32294 | 2.91873 | -0.52010 |
| H | 3.03614 | -5.06768 | 1.61681 |
| H | 5.27360 | 0.23558 | 0.88242 |
| H | -0.08684 | -0.24363 | 1.34237 |
| H | 1.66524 | 2.85732 | 1.69674 |
| H | -4.88175 | -1.19384 | 1.78927 |
| H | -6.27179 | 3.74209 | 1.82398 |
| H | 6.37003 | 0.62604 | 3.05904 |
| H | -3.43273 | -4.87962 | 3.44902 |
| H | -5.25123 | -3.20925 | 3.16494 |
| H | -4.63360 | 2.78344 | 3.43205 |
| H | 2.61720 | 0.01097 | 5.06635 |
| N | 0.15435 | -0.71498 | -1.59687 |
| P | -2.53880 | -0.27238 | 0.16982 |

## 6) Crystallographic Data

Crystal data and details of the structure determinations are compiled in Tables S1-S4. Full shells of intensity data were collected at low temperature with a Bruker AXS Smart 1000 CCD diffractometer (Mo-$K_\alpha$ radiation, sealed X-ray tube, graphite monochromator, complex $^{[B]}$**2-Zr**·1.5 $CH_2Cl_2$) or an Agilent Technologies Supernova-E CCD diffractometer (Mo- or Cu-$K_\alpha$ radiation, microfocus X-ray tube, multilayer mirror optics, all other compounds). Detector frames (typically ω-, occasionally φ-scans, scan width 0.4...1°) were integrated by profile fitting.[6,7,8] Data were corrected for air and detector absorption, Lorentz and polarization effects[7,8] and scaled essentially by application of appropriate spherical harmonic functions.[9,10,11] Absorption by the crystal was treated with a semiempirical multiscan method (as part of the scaling process) augmented by a spherical correction (complex $^{[B]}$**2-Zr**·1.5 $CH_2Cl_2$) ,[10] or numerically (Gaussian grid, all other compounds).[8,11,12,] For datasets collected with the microfocus tubes an illumination correction was performed as part of the numerical absorption correction.[8] The structures were solved by dual-space methods employing the VLD scheme (complex $^{[A]}$**10-Zr**·solv)[13,14] or by the charge flip procedure[15] (all other compounds) and refined by full-matrix least squares methods based on $F^2$ against all unique reflections.[16] All non-hydrogen atoms were given anisotropic displacement parameters.

Hydrogen atoms were generally input at calculated positions and refined with a riding model. When justified by the quality of the data the positions of some hydrogen atoms (typically those with chemical significance, *e.g.* hydrides, agostic interactions or those on π-coordinated arenes) were taken from difference Fourier syntheses and refined. In addition, likely positions for the terminal hydride ligands as well as for the agostic BHZr and CHZr hydrogens in $^{[A]}$**10-Zr** were calculated in turn by minimization of repulsive interactions[17] with the rest of the ligand shell around Zr, while maintaining sensible Zr−H and B−H, C−H distances. The so obtained hydrogen positions of minimum potential energy were then refined simultaneously to include potential hydrogen hydrogen repulsions.[18] The final positions agreed reasonably with those obtained from refinement against the diffraction data (within 0.14 Å (ZrH); 0.11, 0.13 Å (BH); 0.18...0.29 Å (CH)).

When found necessary, disordered groups and/or solvent molecules were subjected to suitable geometry and adp restraints or constraints.

Due to severe disorder and fractional occupancy, some or all electron density attributed to solvent of crystallization was removed from the structures of **[B]ZrCl$_3$** (pentane), $^{[B]}$**4-Zr** (diethyl ether and toluene), $^{B]}$**6-Zr** (diethyl ether) and $^{[A]}$**10-Zr** (toluene and/or benzene, *n*-pentane) with the BYPASS procedure,[19] as implemented in PLATON (squeeze/hybrid).[20] Partial structure factors from the solvent masks were included in the refinement as separate contributions to $F_{calc}$.

Crystals of $^{[B]}$**2-Hf**·toluene were twinned (twin fractions about 83:17). After de-twinning,[8] refinement was carried out against all singles involving the major domain.

CCDC 1530465-1530475 contains the supplementary crystallographic data for this paper. These data can be obtained free of charge from The Cambridge Crystallographic Data Centre via https://www.ccdc.cam.ac.uk/data_request/cif.

Table S1: Details of the crystal structure determinations of [**B**]H, $^{[B]}$**1-Hf** and [**B**]$ZrCl_3$.

| compound | [**B**]H | $^{[B]}$**1-Hf** | **[B]$ZrCl_3$·0.75 pentane** |
|---|---|---|---|
| Formula | $C_{38}H_{33}NP_2$ | $C_{44}H_{50}HfN_4P_2$ | $C_{41.75}H_{41}Cl_3NP_2Zr$ |
| $M_r$ | 565.59 | 875.31 | 816.26 |
| crystal system | triclinic | triclinic | triclinic |
| space group | *P* -1 | *P* -1 | *P* -1 |
| *a* /Å | 10.66534(12) | 12.47419(13) | 11.44486(13) |
| *b* /Å | 12.26799(17) | 12.67913(18) | 17.6843(2) |
| *c* /Å | 13.52930(18) | 14.64329(19) | 19.9828(3) |
| $\alpha$ /° | 111.4620(12) | 81.2172(11) | 80.0131(11) |
| $\beta$ /° | 107.2399(11) | 85.5974(9) | 88.4840(10) |
| $\gamma$ /° | 96.1928(10) | 61.4891(12) | 72.8933(10) |
| *V* /Å$^3$ | 1526.14(4) | 2011.26(5) | 3805.61(8) |
| *Z* | 2 | 2 | 4 |
| $F_{000}$ | 596 | 888 | 1678 |
| $d_c$ /Mg·m$^{-3}$ | 1.231 | 1.445 | 1.425 |
| X-radiation, $\lambda$ /Å | Mo- $K_\alpha$, 0.71073 | Mo- $K_\alpha$, 0.71073 | Cu- $K_\alpha$, 1.54184 |
| $\mu$ /mm$^{-1}$ | 0.170 | 2.708 | 5.332 |
| max., min. transmission factors | 0.979, 0.973 | 0.863, 0.757 | 0.798, 0.560 |
| data collect. temperature /K | 120(1) | 120(1) | 120(1) |
| $\theta$ range /° | 3.3 - 29.1 | 3.2 - 32.4 | 3.8 to 70.8 |
| index ranges (indep. set) *h*,*k*,*l* | ±14, ±16, ±18 | ±18, ±19, ±21 | ±14, ±21, ±24 |
| reflections measured | 161760 | 128166 | 219388 |
| unique [$R_{int}$] | 7949 [0.0628] | 13994 [0.0388] | 14522 [0.0374] |
| observed [$I \geq 2\sigma(I)$] | 7293 | 12875 | 13711 |
| parameters refined [restraints] | 373 [0] | 466 [0] | 811 [0] |
| GooF on $F^2$ | 1.187 | 1.104 | 1.052 |
| *R* indices [$F>4\sigma(F)$] $R(F)$, $wR(F^2)$ | 0.0520, 0.1049 | 0.0237, 0.0514 | 0.0251, 0.0601 |
| *R* indices (all data) $R(F)$, $wR(F^2)$ | 0.0598, 0.1078 | 0.0285, 0.0527 | 0.0272, 0.0610 |
| diff. density: max, min /e·Å$^{-3}$ | 0.408, -0.280 | 1.360, -0.748 | 0.745, -0.645 |
| deposition number CCDC | 1530465 | 1530466 | 1530467 |

Table S2: Details of the crystal structure determinations of $^{[A]}$**2-Zr**, $^{[B]}$**2-Zr** and $^{[B]}$**2-Hf**.

| Compound | $^{[A]}$**2-Zr · 1.5 $CH_2Cl_2$** | $^{[B]}$**2-Zr · $CH_2Cl_2$** | $^{[B]}$**2-Hf · toluene** |
|---|---|---|---|
| Formula | $C_{39.5}H_{35}Cl_3I_3NP_2Zr$ | $C_{39}H_{34}Cl_2I_3NP_2Zr$ | $C_{45}H_{40}HfI_3NP_2$ |
| $M_r$ | 1163.89 | 1121.43 | 1215.91 |
| crystal system | triclinic | monoclinic | monoclinic |
| space group | *P* -1 | *P* $2_1/n$ | *P* $2_1/n$ |
| *a* /Å | 12.32855(16) | 12.220(5) | 12.3761(2) |
| *b* /Å | 12.57691(19) | 16.920(7) | 17.07238(16) |
| *c* /Å | 15.78601(14) | 19.864(9) | 20.1630(3) |
| $\alpha$ /° | 104.1686(10) | | |
| $\beta$ /° | 96.0145(9) | 106.052(10) | 101.9429(13) |
| $\gamma$ /° | 116.0700(14) | | |
| *V* /Å$^3$ | 2067.44(5) | 3947(3) | 4168.04(10) |
| *Z* | 2 | 4 | 4 |
| $F_{000}$ | 1118 | 2152 | 2312 |
| $d_c$ /Mg·m$^{-3}$ | 1.870 | 1.887 | 1.938 |
| X-radiation, $\lambda$ /Å | Mo- $K_\alpha$, 0.71073 | Mo- $K_\alpha$, *0*.71073 | Mo- $K_\alpha$, *0*.71073 |
| $\mu$ /mm$^{-1}$ | 2.806 | 2.871 | 4.834 |
| max., min. transmission factors | 1.000, 0.522 | 0.4950, 0.4342 | 0.912, 0.717 |
| data collect. temperature /K | 120(1) | 100(1) | 120(1) |
| $\theta$ range /° | 2.6 - 29.1 | 1.6 - 32.5 | 2.9 - 32.4 |
| index ranges (indep. set) *h*,*k*,*l* | ±16, ±17, ±21 | ±18, ±24, ±29 | ±18, ±25, ±29 |
| reflections measured | 146604 | 100238 | 111112 |
| unique [$R_{int}$] | 10645 [0.0402] | 13638 [0.0364] | 14368 [0.0639] |
| observed [$I \geq 2\sigma(I)$] | 9648 | 11834 | 10980 |
| parameters refined [restraints] | 479 [7] | 461 [37] | 470 [0] |
| GooF on $F^2$ | 1.043 | 1.045 | 1.161 |
| *R* indices [$F>4\sigma(F)$] $R(F)$, $wR(F^2)$ | 0.0221, 0.0456 | 0.0300, 0.0500 | 0.0404, 0.0917 |
| *R* indices (all data) $R(F)$, $wR(F^2)$ | 0.0271, 0.0471 | 0.0223, 0.0470 | 0.0604, 0.0946 |
| diff. density: max, min /e·Å$^{-3}$ | 0.951, −0.673 | 0.721, -0.602 | 2.483, -1.400 |
| deposition number CCDC | 1530468 | 1530469 | 1530470 |

Table S3: Details of the crystal structure determinations of $^{[B]}$**4-Zr**, $^{[B]}$**5-Zr** and $^{[B]}$**5-Hf**.

| Compound | $^{[B]}$**4-Zr · solv** | $^{[B]}$**5-Zr · OEt$_2$** | $^{[B]}$**5-Hf · OEt$_2$** |
|---|---|---|---|
| Formula | $C_{52}H_{45}NP_2Zr$ | $C_{49}H_{48}ClNOP_2Zr$ | $C_{49}H_{48}ClHfNOP_2$ |
| $M_r$ | 837.05 | 855.49 | 942.76 |
| crystal system | monoclinic | monoclinic | monoclinic |
| space group | *P* $2_1/n$ | *P* $2_1/c$ | *P* $2_1/c$ |
| *a* /Å | 14.04739(15) | 12.1149(2) | 12.05585(7) |
| *b* /Å | 12.35375(14) | 12.1996(2 | 12.17458(6) |
| *c* /Å | 28.0234(3) | 28.4817(4) | 28.6103(2) |
| $\alpha$ /° | | | |
| $\beta$ /° | 98.1365(10) | 91.1112(15) | 91.9077(6) |
| $\gamma$ /° | | | |
| *V* /Å$^3$ | 4814.18(9) | 4208.73(12) | 4196.94(4) |
| *Z* | 4 | 4 | 4 |
| $F_{000}$ | 1736 | 1776 | 1904 |
| $d_c$ /Mg·m$^{-3}$ | 1.155 | 1.350 | 1.492 |
| X-radiation, $\lambda$ /Å | Mo-$K_\alpha$, *0*.71073 | Mo-$K_\alpha$, *0*.71073 | Cu- $K_\alpha$, 1.54184 |
| $\mu$ /mm$^{-1}$ | 0.327 | 0.438 | 6.187 |
| max., min. transmission factors | 0.979, 0.947 | 0.975, 0.960 | 0.738, 0.628 |
| data collect. temperature /K | 120(1) | 120(1) | 120(1) |
| $\theta$ range /° | 2.9 - 32.3 | 3.2 - 30.6 | 3.7 - 70.9 |
| index ranges (indep. set) *h*,*k*,*l* | ±20, ±18, -42 …41 | ±17, ±17, ±40 | ±14, ±14, -32 … 35 |
| reflections measured | 169444 | 106852 | 179970 |
| unique [$R_{int}$] | 16744 [0.0651] | 12873 [0.0825] | 8028 [0.0411] |
| observed [$I \geq 2\sigma(I)$] | 15033 | 9920 | 7722 |
| parameters refined [restraints] | 526 [0] | 501 [24] | 501 [24] |
| GooF on $F^2$ | 1.190 | 1.032 | 1.118 |
| *R* indices [$F>4\sigma(F)$] $R(F)$, $wR(F^2)$ | 0.0553, 0.1086 | 0.0470, 0.1104 | 0.0288, 0.0693 |
| *R* indices (all data) $R(F)$, $wR(F^2)$ | 0.0643, 0.1118 | 0.0677, 0.1204 | 0.0303, 0.0700 |
| diff. density: max, min /e·Å$^{-3}$ | 0.991, -1.260 | 1.816, -0.756 | 1.411, -0.706 |
| deposition number CCDC | 1530471 | 1530472 | 1530473 |

Table S4: Details of the crystal structure determinations of $^{[B]}$**6-Zr** and $^{[B]}$**10-Zr**.

| Compound | $^{[B]}$**6-Zr · 0.5 OEt$_2$** | $^{[A]}$**10-Zr · solv** [a] |
|---|---|---|
| formula | $C_{47}H_{45}ClNO_{0.5}P_2Zr$ | $C_{62}H_{70}BNP_2Zr$ |
| $M_r$ | 820.45 | 993.16 |
| crystal system | monoclinic | triclinic |
| space group | *I* 2/*a* | P -1 |
| *a* /Å | 18.9791(3) | 17.3823(5) |
| *b* /Å | 11.12020(16) | 17.7265(5) |
| *c* /Å | 38.2266(5) | 21.7567(5) |
| $\alpha$ /° | | 67.552(2) |
| $\beta$ /° | 101.1276(14) | 66.932(2) |
| $\gamma$ /° | | 66.047(3) |
| *V* /Å$^3$ | 7916.1(2) | 5435.2(3) |
| *Z* | 8 | 4 |
| $F_{000}$ | 3400 | 2096 |
| $d_c$ /Mg·m$^{-3}$ | 1.377 | 1.214 |
| X-radiation, $\lambda$ /Å | Mo-$K_\alpha$, 0.71073 | Mo-$K_\alpha$, 0.71073 |
| $\mu$ /mm$^{-1}$ | 0.462 | 0.300 |
| max., min. transmission factors | 0.991, 0.959 | 0.984, 0.950 |
| data collect. temperature /K | 120(1) | 120(1) |
| $\theta$ range /° | 3.0 - 32.3 | 2.6 - 30.6 |
| index ranges (indep. set) *h*,*k*,*l* | ±28, -16 ... 15, ±57 | ±24, ±25, ±31 |
| reflections measured | 125681 | 243662 |
| unique [$R_{int}$] | 13622 [0.0562] | 33234 [0.0928] |
| observed [$I \geq 2\sigma(I)$] | 11129 | 23925 |
| parameters refined [restraints] | 467 [2] | 1035 [57] |
| GooF on $F^2$ | 1.024 | 1.041 |
| *R* indices [$F>4\sigma(F)$] $R(F)$, $wR(F^2)$ | 0.0342, 0.0759 | 0.0506, 0.1148 |
| *R* indices (all data) $R(F)$, $wR(F^2)$ | 0.0479, 0.0810 | 0.0758, 0.1247 |
| diff. density: max, min /e·Å$^{-3}$ | 1.483, -0.404 | 1.394, −0.525 |
| deposition number CCDC | 1530474 | 1530475 |

[a] solv = pentane, benzene and toluene

## 7) References


[1] M. J. Frisch, G. W. Trucks, H. B. Schlegel, G. E. Scuseria, M. A. Robb, J. R. Cheeseman, J. A. Montgomery, T. Vreven, K. N. Kudin, J. C. Burant, J. M. Millam, S. S. Iyengar, J. Tomasi, V. Barone, B. Mennucci, M. Cossi, G. Scalmani, N. Rega, G. A. Petersson, H. Nakatsuji, M. Hada, M. Ehara, K. Toyota, R. Fukuda, J. Hasegawa, M. Ishida, T. Nakajima, Y. Honda, O. Kitao, H. Nakai, M. Klene, X. Li, J. E. Knox, H. P. Hratchian, J. B. Cross, V. Bakken, C. Adamo, J. Jaramillo, R. Gomperts, R. E. Stratmann, O. Yazyev, A. J. Austin, R. Cammi, C. Pomelli, J. W. Ochterski, P. Y. Ayala, K. Morokuma, G. A. Voth, P. Salvador, J. J. Dannenberg, V. G. Zakrzewski, S. Dapprich, A. D. Daniels, M. C. Strain, O. Farkas, D. K. Malick, A. D. Rabuck, K. Raghavachari, J. B. Foresman, J. V. Ortiz, Q. Cui, A. G. Baboul, S. Clifford, J. Cioslowski, B. B. Stefanov, G. Liu, A. Liashenko, P. Piskorz, I. Komaromi, R. L. Martin, D. J. Fox, T. Keith, A. Laham, C. Y. Peng, A. Nanayakkara, M. Challacombe, P. M. W. Gill, B. Johnson, W. Chen, M. W. Wong, C. Gonzalez and J. A. Pople, *Gaussian 03, Revision C.02*, **2003**.

[2] (a) A. D. Becke, *J. Chem. Phys.* **1993**, *98*, 564; (b) K. Burke, J. P. Perdew and Y. Wang, In *Electronic Density Functional Theory: Recent Progress and New Directions,* J. F. Dobson, G. Vignale and M. P. Das (Eds.), Plenum Press: New York, **1998**; (c) J. P. Perdew, *Phys. Rev. B* **1986**, *33*, 8822.

[3] (a) B. Metz, H. Stoll and M. J. Dolg, *Chem. Phys.* **2000**, *113*, 2563; (b) M. Dolg, U. Wedig, H. Stoll and H. Preuss, *J. Chem. Phys.* **1987**, *86*, 866.

[4] (a) P. C. Hariharan and J. A. Pople, *Theor. Chim. Acta* **1973**, *28*, 213; (b) R. Krishnan, J. S. Binkley, R. Seeger and J. A. Pople *J. Chem. Phys.* **1980**, *72*, 650.

[5] (a) E. D. Glendening, A. E. Reed, J. E. Carpenter and F. Weinhold, *NBO Version 3.1*; (b) J. P. Foster and F. Weinhold, *J. Am. Chem. Soc.* **1980**, *102*, 7211.

[6] K. Kabsch, In *International Tables for Crystallography*, M. G. Rossmann and E. Arnold (Eds.), *Vol. F*, Ch. 11.3, Kluwer Academic Publishers: Dordrecht, **2001**.

[7] *SAINT*, Bruker AXS GmbH, Karlsruhe, Germany **1997-2013**.

[8] (a) *CrysAlisPro*, Agilent Technologies UK Ltd., Oxford, UK **2011**-**2014**; (b) Rigaku Oxford Diffraction, Rigaku Polska Sp.z o.o., Wrocław, Poland **2015**-**2016**.

[9] R. H. Blessing, *Acta Cryst.* **1995**, *A51*, 33.

[10] (a) G. M. Sheldrick, *SADABS*, Bruker AXS GmbH, Karlsruhe, Germany **2004-2014**; (b) L. Krause, R. Herbst-Irmer, G. M. Sheldrick and D. Stalke, *J. Appl. Cryst.* **2015**, *48*, 3.

[11] (a) *SCALE3 ABSPACK, CrysAlisPro*, Agilent Technologies UK Ltd., Oxford, UK **2011**-**2014**; (b) Rigaku Oxford Diffraction, Rigaku Polska Sp.z o.o., Wrocław, Poland **2015**-**2016**.

[12] W. R. Busing and H. A. Levy, *Acta Cryst.* **1957**, *10*, 180.

[13] M. C. Burla, C. Giacovazzo and G. Polidori, *J. Appl. Cryst.* **2010**, *43*, 825.

[14] (a) M. C. Burla, R. Caliandro, B. Carrozzini, G. L. Cascarano, C. Cuocci, C. Giacovazzo, M. Mallamo, A. Mazzone and G. Polidori, *SIR2014*, CNR IC, Bari, Italy, **2014**; (b) M. C. Burla, R. Caliandro, B. Carrozzini, G. L. Cascarano, C. Cuocci, C. Giacovazzo, M. Mallamo, A. Mazzone and G. Polidori, *J. Appl. Cryst.* **2015**, *48*, 306.

[15] (a) L. Palatinus, *SUPERFLIP*, EPF Lausanne, Switzerland and Fyzikální ústav AV ČR, v. v. i., Prague, Czech Republic, **2007**-**2014**; (b) L. Palatinus and G. Chapuis, *J. Appl. Cryst.* **2007**, 40, 786.

[16] (a) G. M. Sheldrick, *SHELXL-20xx*, University of Göttingen and Bruker AXS GmbH, Karlsruhe, Germany **2012**-**2016**; (b) G. M. Sheldrick, *Acta Cryst.* **2008**, *A64*, 112; (c) G. M. Sheldrick, *Acta Cryst.* **2015**, *C71*, 3.

[17] G. Filippini and A. Gavezzotti, *Acta Cryst.* **1993**, *B49*, 868.

[18] (a) A. G. Orpen, *HYDEX*, University of Bristol, UK, **1986**; (b) A. G. Orpen, *J. Chem. Soc., Dalton Trans.* **1980**, 2509.

[19] (a) P. v. d. Sluis and A. L. Spek, *Acta Cryst.* **1990**, *A46*, 194; (b) A. L. Spek, *Acta Cryst.* **2015**, *C71*, 9.

[20] (a) A. L. Spek, *PLATON*, Utrecht University, The Netherlands; (b) A. L. Spek, *J. Appl. Cryst*. **2003**, *36*, 7.